

**MECHANICAL AND THERMAL PROPERTIES OF  
NON-CRIMP GLASS FIBER REINFORCED  
COMPOSITES WITH SILICATE  
NANOPARTICULE MODIFIED EPOXY MATRIX**

**A Thesis submitted to  
the Graduate School of Engineering and Science of  
Izmir Institute of Technology  
in Partial Fulfillment of the Requirements for the Degree of**

**MASTER OF SCIENCE**

**in Mechanical Engineering Department**

**by  
Emrah BOZKURT**

**July 2006  
Izmir, Turkey**

We approve the thesis of **Emrah BOZKURT**

**Date of Signature**

.....

**17 July 2006**

**Assoc. Prof. Dr. Metin TANOĞLU**  
Supervisor  
Department of Mechanical Engineering  
Izmir Institute of Technology

.....

**17 July 2006**

**Assoc. Prof. Dr. Mustafa GÜDEN**  
Department of Mechanical Engineering  
Izmir Institute of Technology

.....

**17 July 2006**

**Assoc. Prof. Dr. Talal SHAHWAN**  
Department of Chemistry  
Izmir Institute of Technology

.....

**17 July 2006**

**Assoc. Prof. Dr. Barış ÖZERDEM**  
Head of Department  
Izmir Institute of Technology

.....

**Assoc. Prof. Dr. Semahat Özdemir**  
Head of the Graduate School

## **ACKNOWLEDGEMENT**

I am very grateful to my supervisor Assoc. Prof. Metin Tanođlu for his immense help, guidance, support and encouragement throughout my study. I would like to acknowledge Telateks A.Ş. and Enercon Aero A.Ş. for their support and The Scientific and Technical Research Council of Turkiye (TUBİTAK) for financial support to 104M365 project. I would like to thank İYTE-MAM personals for their helps during my material characterization studies.

I want to express my appreciation to all my friends and especially I wish to thank Kıvanç Işık, Elçin Dilek Kaya and Anıl Coşkun for their help, assistance and friendship. With a deep sense of gratitude, I wish to express my sincere thanks to my family and Esra Kayagil for their unlimited support and motivation in every steps of my study.

## ABSTRACT

### MECHANICAL AND THERMAL PROPERTIES OF NON-CRIMP GLASS FIBER REINFORCED COMPOSITES WITH SILICATE NANOPARTICULE MODIFIED EPOXY MATRIX

In the present study, epoxy based nanocomposites were prepared with modified and unmodified silicate nanoparticles to apply as a matrix resin for non-crimp glass fiber reinforced polymer composites. The effects of the silicate nanoparticles on the mechanical, thermal and flame retardancy properties of glass reinforced composites were investigated. Laminates were manufactured with hand lay-up technique and cured under compression. To intercalate the layers and obtain better dispersion of silicate layers within the matrix, silicate (montmorillonite, MMT) particles were treated with hexadecyltrimethylammonium chloride (HTAC) surfactants. X-ray diffraction of silicates with and without surface treatment indicated that intergallery spacing of layered silicate increased with surface treatment. Tensile tests showed that silicate loading had minor effect on the tensile strength and modulus of the composite laminates. Flexural properties of laminates were improved with the addition of silicate due to the improved interface between glass fibers and epoxy matrix. With the addition of modified MMT (OMMT), interlaminar shear strength (ILSS) of laminates decreased slightly but fracture toughness ( $K_{IC}$ ) of laminates were increased. The fracture surfaces were examined with scanning electron microscopy (SEM) and the results revealed that fracture mechanisms were altered due to the presence of silicates in the matrix. Differential scanning calorimetry (DSC) results showed that modified silicate particles increase the glass transition temperatures ( $T_g$ ) of composite laminates. Incorporation of OMMT particles increased the dynamic mechanical properties of non-crimp glass fiber reinforced epoxy composites. It was found that the flame resistance of composites was improved due to silicate particule additions into the epoxy matrix.

## ÖZET

### SİLİKA NANOPARTİKÜLLER İLE MODİFİYE EDİLMİŞ EPOKSİ MATRİKSLİ KIVRIMSIZ FİBER TAKVİYELİ KOMPOZİTLERİN MEKANİK VE TERMAL ÖZELLİKLERİ

Bu çalışmada, kıvrımsız cam fiberlerle güçlendirilmiş polimer kompozitlerin matriksi olarak kullanılmak üzere modifiye edilmiş ve edilmemiş silika nanopartiküller ile epoksi bazlı nanokompozitler hazırlanmıştır. Silika nanopartiküllerinin, cam takviyeli kompozitlerin mekanik, termal ve yanma özelliklerine etkisi araştırılmıştır. Kompozitler el yatırması yöntemi ile üretilmiş ve basınç altında kürlenmiştir. Silika tabakaları arası mesafeyi artırma ve matriks içinde daha iyi dağılmalarını sağlamak amacı ile silika (montmorillonit, MMT) partikülleri hexadecyltrimethylammonium chloride (HTAC) yüzey aktif maddesi ile kimyasal işleme tabi tutulmuştur. Modifiye edilmiş ve edilmemiş silika partiküllerinin X-ışınımı kırınımı test sonuçları, tabakalı silikaların galeriler arası boşluk mesafesinin modifikasyon ile arttığını göstermiştir. Çekme testi sonuçları kil takviyesinin kompozitlerin çekme mukavemeti ve modülüne çok az bir etkisi olduğunu göstermektedir. Kompozitlerin eğme özellikleri, silika eklenmesiyle iyileşen cam fiber-epoksi matriks ara yüzüne bağlı olarak gelişmiştir. Silika takviyesi, kompozitlerin laminalar arası kayma mukavemetini (ILSS) düşürmekte fakat kompozitlerin kırılma tokluğunu ( $K_{IC}$ ) arttırmaktadır. Taramalı elektron mikroskobu ile kırılma yüzeyleri incelenmiştir ve sonuçlar matriksin içindeki silika partiküllerinin varlığının kırılma mekanizmalarını değiştirdiğini göstermiştir. Diferansiyel taramalı kalorimetre (DSC) sonuçları modifiye edilmiş kil partiküllerinin kompozitlerin camsı geçiş sıcaklıklarını ( $T_g$ ) bir miktar arttırdığını göstermiştir. Modifiye edilmiş silika partiküllerinin eklenmesi ile kompozitlerin dinamik mekanik özelliklerinde artış gözlenmiştir. Kompozitlerin yanma geciktirme özelliğinin epoksi matrikse silika partikülleri eklenmesi ile geliştiği gözlenmiştir.

# TABLE OF CONTENTS

LIST OF FIGURES .....	ix
LIST OF TABLES .....	xii
CHAPTER 1. INTRODUCTION.....	1
CHAPTER 2. FIBER REINFORCED POLYMER COMPOSITES .....	3
2.1. Structure of Composites.....	3
2.2. Mechanical Behaviour of Polymer Matrix Composites .....	9
2.3. Non-Crimp Fabric Reinforced Composites .....	11
CHAPTER 3. NANOPARTICULATE FILLED COMPOSITES .....	15
3.1. Layered Silicates .....	15
3.2. Modification of Layered Silicates .....	16
3.3. Layered Silicate/Polymer Nanocomposites .....	18
3.3.1. Melt Intercalation .....	18
3.3.2. Solution Method.....	19
3.3.3. In-situ Polymerization .....	19
3.4. Morphology of Layered Silicate/Polymer Nanocomposites.....	19
3.5. Properties of Nanocomposites .....	21
3.6. Nanofiller Added Fabric Reinforced Composites .....	28
CHAPTER 4. FIBER REINFORCED POLYMER COMPOSITE MANUFACTURING METHODS .....	32
4.1. Hand Lay-up .....	32
4.2. Resin Transfer Molding .....	34
4.3. Vacuum Assisted Resin Transfer Molding.....	35
4.4. Compression Molding.....	37
CHAPTER 5. EXPERIMENTAL .....	39
5.1. Materials .....	39

5.2. Surface Modification of Montmorillonite Clay .....	39
5.3. Preparation of Layered Silicate/Epoxy Suspension .....	40
5.4. Composite Fabrication .....	40
5.5. Fiber Volume Fraction.....	41
5.6. Microstructure Characterization .....	42
5.6.1. X-Ray Diffraction (XRD) .....	42
5.6.2. Scanning Electron Microscopy (SEM) .....	42
5.6.3. Optical Microscopy .....	43
5.7. Mechanical Property Characterization.....	43
5.7.1. Tensile Test .....	43
5.7.2. Flexural Test.....	44
5.7.3. Short Beam Shear (SBS) Test .....	46
5.7.4. Fracture Toughness ( $K_{IC}$ ) Test .....	47
5.8. Thermal Property Characterization.....	48
5.8.1. Differential Scanning Calorimetry (DSC).....	48
5.8.2. Dynamic Mechanical Analysis (DMA).....	48
5.8.3. Flame Retardancy.....	49
CHAPTER 6. RESULTS AND DISCUSSION .....	51
6.1. Fiber Volume Fraction and Void Content .....	51
6.2. Microstructural Development.....	53
6.3. Effects of Silicate Layers on the Mechanical Properties of the Composites.....	55
6.3.1. Tensile Properties.....	55
6.3.2. Flexural Properties .....	58
6.3.3. Interlaminar Shear Strength (ILSS).....	62
6.3.4. Fracture Toughness ( $K_{IC}$ ).....	63
6.4. Thermal Properties.....	64
6.4.1. Effect of Silicate Loading on the Glass Transition Temperature of Laminates .....	64
6.4.2. Effect of Silicate Loading on the Thermomechanical Properties of Laminates.....	66
6.5. Flammability Behaviour of Composites .....	70

CHAPTER 7. CONCLUSIONS.....	73
REFERENCES .....	75

## LIST OF FIGURES

<b><u>Figure</u></b>	<b><u>Page</u></b>
Figure 2.1. Classification scheme of composite materials .....	4
Figure 2.2 Particle-reinforced composites .....	4
Figure 2.3. Form and orientation of the fibers in fiber reinforced composites .....	5
Figure 2.4. Schematic illustration of NCFs.....	13
Figure 2.5. Resin pockets in a composite manufactured with woven fabrics .....	13
Figure 2.6. Laminate prepared with NCFs.....	13
Figure 3.1. The structure of 2:1 layered silicates .....	16
Figure 3.2. Schematic representation of clay surface treatment .....	17
Figure 3.3. Morphologies of polymer/clay nanocomposites.....	20
Figure 3.4. SEM micrographs of fracture surfaces of (a) epoxy/ 3 wt. % MMT (b) epoxy/ 3 wt. % OMMT nanocomposites .....	23
Figure 3.5. (a) Tensile modulus and (b) tensile strength of silicate/epoxy nanocomposites.....	24
Figure 3.6. Tensile modulus of epoxy/clay nanocomposites at varied clay concentrations .....	24
Figure 3.7. Tensile strength of epoxy/clay nanocomposites at varied clay concentrations.....	25
Figure 3.8. Elongation at break of epoxy/clay nanocomposites at varied clay concentrations .....	25
Figure 3.9. SEM micrographs of fracture surfaces of nanocomposites made with the DDM .....	26
Figure 3.10. DSC thermograms of epoxy/clay nanocomposites (a) no clay addition (b) 20 phr MMT (c) 5 phr OMMT (d) 20 phr OMMT .....	27
Figure 3.11. Formation of tortuous path in nanocomposites.....	27
Figure 3.12. Relationship between (a) aspect ratio and relative permeability (b) clay loading and relative permeability for a clay with an aspect ratio of 250.....	28
Figure 3.13. Compressive strength results of fiber reinforced composites .....	29
Figure 3.14. Flow patterns with different fiber directions; (a) transverse direction; (b) longitudinal direction.....	30

Figure 4.1.	Schematic illustration of hand-lay up .....	32
Figure 4.2.	Schematic illustration of RTM .....	35
Figure 4.3.	Schematic illustration of VARTM process.....	36
Figure 4.4.	Schematic illustration of preform molding .....	37
Figure 5.1.	Surface treatment route for montmorillonite.....	40
Figure 5.2.	Flowchart of composite fabrication process .....	41
Figure 5.3.	Tensile test specimen under load .....	44
Figure 5.4.	Flexural testing specimen under loading.....	45
Figure 5.5.	SBS test configuration .....	46
Figure 5.6.	Fracture toughness test specimen .....	47
Figure 5.7.	Horizontal burn set up.....	49
Figure 6.1.	Optical micrographs of (a) NCF/neat epoxy composites (b) NCF/3 wt.% OMMT/epoxy composites .....	52
Figure 6.2.	Optical micrographs of (a) NCF/ neat epoxy composite (b) NCF/3 wt.% OMMT/epoxy composites transformed to binary images .....	52
Figure 6.3.	X-ray diffractograms of MMT and OMMT silicates.....	53
Figure 6.4.	X-ray diffractograms of glass fiber reinforced MMT/epoxy nanocomposites .....	54
Figure 6.5.	X-ray diffractograms of glass fiber reinforced OMMT/epoxy.....	54
Figure 6.6.	Tensile stress vs. strain response of composites with and without MMT loading.....	55
Figure 6.7.	Tensile stress vs. strain response of composites with and without OMMT loading .....	56
Figure 6.8.	Tensile strength of non-crimp glass fabric reinforced epoxy composites with silicate nanoparticle addition .....	57
Figure 6.9.	Elastic modulus of non-crimp glass fabric reinforced epoxy composites with silicate nanoparticle addition .....	57
Figure 6.10.	Flexural stress vs. strain response of composites with MMT loading .....	58
Figure 6.11.	Flexural stress vs. strain response of composites with OMMT loading .....	58
Figure 6.12.	Flexural strength of non-crimp glass fabric reinforced epoxy composites with silicate nanoparticle addition .....	60

Figure 6.13. Flexural modulus of non-crimp glass fabric reinforced epoxy composites with silicate nanoparticle addition .....	60
Figure 6.14. SEM fracture surface images of non-crimp glass fiber/epoxy composites .....	61
Figure 6.15. SEM fracture surface image of non-crimp glass fiber/epoxy composites with 10 wt. % silicate addition.....	61
Figure 6.16. ILSS of non-crimp glass fabric reinforced epoxy composites with silicate nanoparticle addition .....	62
Figure 6.17. Fracture toughness ( $K_{IC}$ ) of non-crimp glass fabric reinforced silicate/epoxy nanocomposites .....	63
Figure 6.18. DSC thermographs of non-crimp glass fabric reinforced MMT/epoxy nanocomposites .....	65
Figure 6.19. DSC thermographs of non-crimp glass fabric reinforced OMMT/epoxy nanocomposites .....	65
Figure 6.20. Storage Modulus versus temperature plots of non-crimp glass fabric reinforced composites prepared with neat epoxy and nanocomposite containing 1 wt.% MMT and OMMT .....	66
Figure 6.21. Loss modulus versus temperature plots of non-crimp glass fabric reinforced composites prepared with neat epoxy and nanocomposite containing 1 wt.% MMT and OMMT .....	67
Figure 6.22. Tan $\delta$ versus temperature plots of non-crimp glass fabric reinforced composites prepared with neat epoxy and nanocomposite containing 1 wt.% MMT and OMMT .....	67
Figure 6.23. Storage modulus of non-crimp fabric reinforced silicate/epoxy nanocomposites.....	68
Figure 6.24. Loss modulus of fabric reinforced silicate/epoxy nanocomposites .....	69
Figure 6.25. $T_g$ of non-crimp fabric reinforced silicate/epoxy nanocomposites obtained by DMA .....	70
Figure 6.26. Influence of silicate loading on the average extent of burning of the non-crimp glass fabric reinforced silicate/epoxy nanocomposites.....	71
Figure 6.27. Influence of silicate loading on the average time of burning of the non-crimp glass fabric reinforced silicate/epoxy nanocomposites .....	72

## LIST OF TABLES

<b><u>Table</u></b>		<b><u>Page</u></b>
Table 2.1.	Glass fiber compositions.....	8
Table 2.2.	Processing Glass fiber properties.....	9
Table 2.3.	Description of advanced textile manufacturing techniques.....	12
Table 6.1.	Fiber volume fraction and void contents of composite laminates fabricated with various type of silicates .....	51

# CHAPTER 1

## INTRODUCTION

Fiber reinforced polymer matrix composites (PMCs) have been widely used in various applications, i.e.; aerospace, defence, automotive, marine and sporting goods due to their high specific stiffness and strength. These materials also provide high durability, design flexibility and lightweight which make them attractive materials in these industrial areas (Tanoğlu et al. 2001, Tarim et al. 2002). The properties of composites are significantly related to the properties of composite constituents, i.e.; matrix, fiber and the interphase between them (Shahid et al. 2005).

The use of nanoclays as fillers in polymer composites has attracted considerable attention due to the improved mechanical, thermal, flame retardant and gas barrier properties of the resulting composites. Because of the extremely high surface to volume ratios and the nanometer size dispersion of nanoclays in polymers, nanocomposites exhibit improved properties as compared to the pure polymers.

Clays used in preparing polymer-clay nanocomposites belong to the 2:1 layered structure. Montmorillonite (MMT) is a layered aluminosilicate in the family of smectite clays. Each layer consists of two sheets of silica tetrahedra with an edge shared octahedral sheet of either alumina (aluminosilicates) or magnesia (magnesium silicates). These layers are held together with a layer of charge-compensating cations such as  $\text{Li}^+$ ,  $\text{Na}^+$ ,  $\text{K}^+$ , and  $\text{Ca}^+$  (Subramanian et al. 2006). Generally the surface of the clay needs to be modified to improve the wettability and dispersibility of hydrophilic clay. The charge-compensating cations can easily be exchanged with surfactants including alkyl ammonium cations. The role of the alkylammonium cations in the organosilicates is to lower the surface energy of the inorganic component and improve the wetting characteristics with the polymer systems. (Giannelis 1998).

Polymer-clay nanocomposites have been synthesized with different approaches: melt intercalation, solution polymerization and in-situ polymerization. In melt intercalation method, a thermoplastic polymer is mechanically mixed with organophilic clay at an elevated temperature. The polymer chains are then intercalated between the individual silicate layers of the clay (Ahmadi et al. 2004). In the solution method, the

polymer and the organoclay are dissolved in a polar organic solvent. The entropy gained by the desorption of solvent molecules allows the polymer chains to diffuse between the clay layers, compensating for their decrease in conformational entropy. After evaporation of the solvent, an intercalated nanocomposite results (Ahmadi et al. 2004, Qutubuddin et al. 2001). In in-situ polymerization technique, nanoscale particles are dispersed in the monomer or monomer solution, and the resulting mixture is polymerized by standard polymerization methods (Qutubuddin et al. 2001).

Non-crimp fabric (NCF) reinforced composites are obtained by stacking blankets which are typically made up from 2 to 4 layers of fibre stitched together through their thickness. Each layer is made up of tows of fibers placed side by side. Damage tolerance of fabric reinforced composites is improved with the use of NCFs. Laminates made up with NCFs show higher compressive strength than woven fabric composites due to the lower waviness in NCF composites (Drapier et al., Zhao et al. 2006). Laminates made up of NCF composites have higher volume fractions and strength since they do not have resin pockets unlike the woven fabrics (Adden et al. 2006).

The objective of this study is to investigate the effect of clay nanoparticles on the mechanical, thermal and flame retardant properties of glass fiber reinforced epoxy composites. A surface treatment process was applied to the clay particles in order to improve the dispersion of silicate layers in epoxy matrix.

In the current research, clay/epoxy nanocomposite systems were used as matrix material with non-crimp glass fabrics. Glass fabrics were impregnated with unmodified (MMT) and modified (OMMT) clay containing epoxy resin to fabricate composite laminates. The clays were intercalated with the matrix resin through in-situ polymerization technique and laminates were polymerized under compression. The structure of clay and clay containing laminates was investigated through X-ray diffraction (XRD) and scanning electron microscopy (SEM). Mechanical, thermal and flammability properties of laminates manufactured with MMT and OMMT containing resin were investigated.

## CHAPTER 2

### FIBER REINFORCED POLYMER COMPOSITES

#### 2.1. Structure of Composites

Many advanced technologies require materials with unusual combinations of properties that can not be met by the conventional metal alloys, ceramics and polymeric materials. The development of composite materials has a role on the material property combinations and ranges. Composite materials are the combinations of two or more distinct materials, having a recognizable interphase between them. In many cases, a strong and stiff component is called fiber is embedded in a softer constituent forming the matrix (Hull and Clyne 1996).

In composites, matrix phase surrounds the reinforcement phase which is also called dispersed phase and acts as a medium by which an externally applied stress is transmitted to the fibers. The properties of composites are the function of the properties of the constituent phases, their relative amounts, and the geometry of the dispersed phase (Tong et al. 2002). The classification scheme of composite materials is shown in Figure 2.1.

Particule reinforced composites are a class of composites as shown in Figure 2.2. Particule and dispersion strenghtened composites are the two sub classifications of this type. For most of these composites, the particulate phase is harder and stiffer than the matrix. Dispersion-strenghtened composites are considered to be perfectly bonded to the matrix and the shape influence of particules is generally neglected. Strenghtening occurs on the atomic or molecular level by particule-matrix interaction. Also, in high performance composite structures, protective coatings may be filled with particulates especially for special properties (eg. abrasive properties) (Stellbrink 1996, Callister 2000).

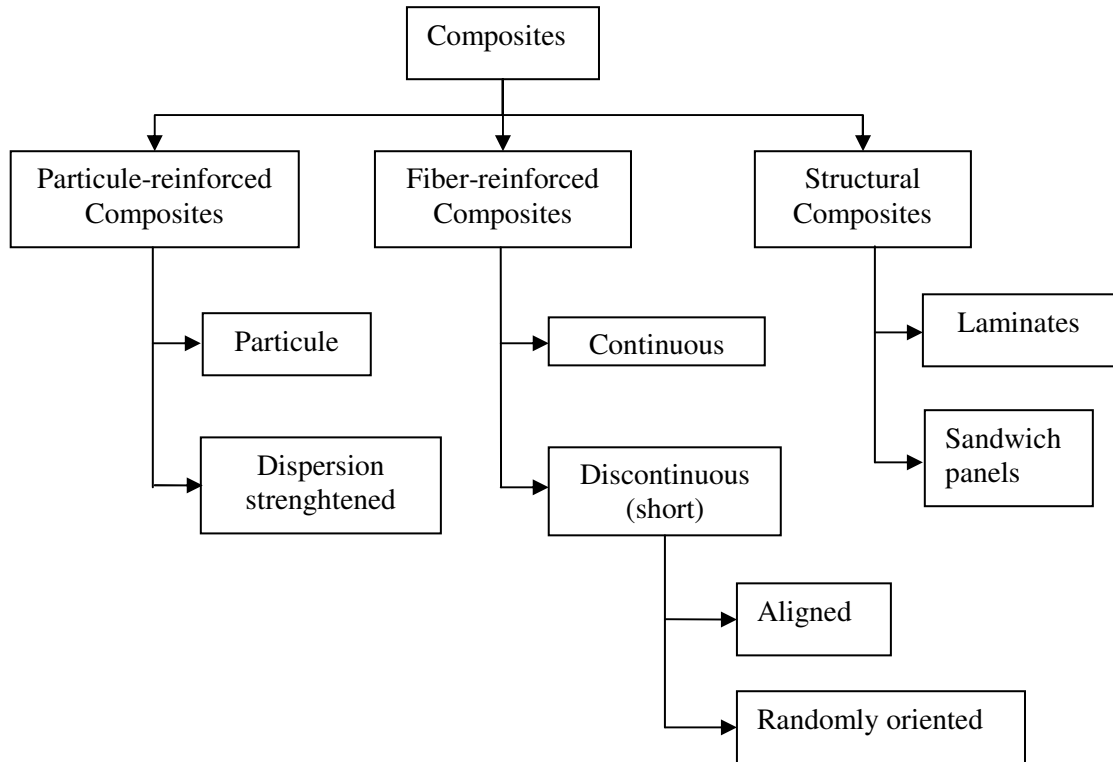


Figure 2.1. Classification scheme of composite materials

(Source: Callister 2000).

The mechanical properties of a fiber reinforced composite depend not only on the properties of the fiber and the matrix, but also on the degree to which an applied load is transmitted to the fibers by the matrix phase (Tong et al. 2002). Therefore; the mechanical properties of the fiber/matrix interface are critical since the load is transferred through the interface region.

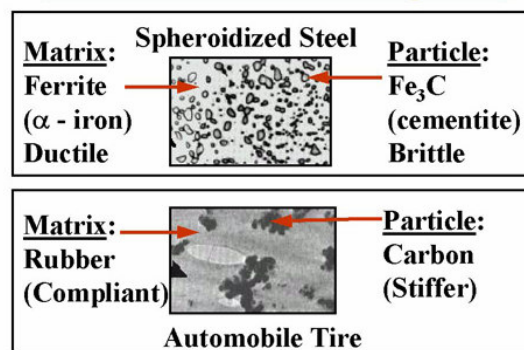


Figure 2.2. Particulate-reinforced composites

(Source: WEB\_1 2006).

The arrangement or orientation of the fibers relative to one another and the fiber concentration and the distribution have significant influences on the properties of fiber reinforced composites. Reinforcement efficiency is also a critical parameter in composites and it is lower in discontinuous fibers as compared to continuous fibers. A variety of form and orientations of the fibers in fiber reinforced composites are shown in Figure 2.3.

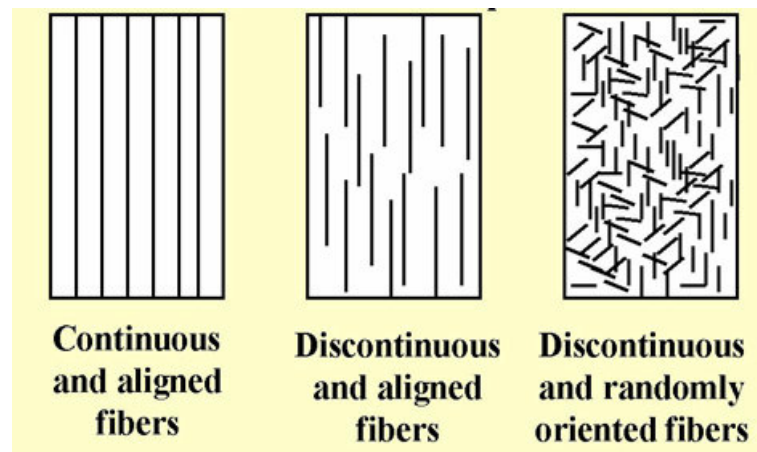


Figure 2.3. Form and orientation of the fibers in fiber reinforced composites

(Source: WEB\_1 2006).

The properties of structural composites depend on the properties of the constituent materials and the geometrical design of the structural elements. The most common structural composites are laminar composites and sandwich panels. A laminar composite is composed of two dimensional sheets or panels which have higher strength in the direction of the continuous fibers.

The matrix of a fibrous composite protects the individual fibers from surface damage including mechanical abrasion and chemical reactions with the environment. It also separates the fibers from each other and prevents the propagation of brittle cracks from fiber to fiber. PMCs consist of a polymer matrix, that can be classified into two groups; thermoplastic and thermoset. Thermoset polymer matrix consists of polymer chains that can be cured into a crosslinked network when mixed with a catalyst, exposed to heat, or both. They are most widely used for composites in both commercial and high performance aerospace applications (Ulven 2003). Curing usually occurs under elevated temperature and/or pressure conditions in an oven and/or vacuum bag or

an autoclave. Alternative curing technologies include electron beam, ultraviolet radiation, X-ray and microwave processes (Dawson et al. 2006, Callister 2000).

Cure of thermoset resins is generally exothermic reaction and they release heat when they crosslink. The curing process is complex due to the interaction between the resin chemistry and variation of physical properties (Kiuna et al. 2002). Cure profile of a thermoset polymer can be controlled in terms of shelf life, pot life, gel time, cure temperature and viscosity through careful formulation of the catalyst package, which may include inhibitors and accelerators. In contrast to crosslinking thermosets, whose cure reaction cannot be reversed, thermoplastics harden when cooled but retain their plasticity. When they are reheated above their processing temperature, they will soften and can be reshaped repeatedly. Thermoplastics are less expensive than thermosets but have limited application temperatures (Dawson et al. 2006).

Unsaturated polyester resins are the most widely used matrix material for the composite industry, because of their easy handling, good mechanical, electrical and chemical properties and relatively low cost (Rouison et al. 2003). They are commonly used in open mold wet lay-up, compression molding, resin transfer molding with glass fiber reinforcements. Specially formulated unreinforced polyester resins improve the impact resistance, abrasion resistance and the surface appearance of the final product. These are applied to a mold surface and gelled before lay up of the composite and called as gel coats.

Vinyl ester resins show better adhesion and fatigue properties than polyester. They also offer a bridge between polyesters and higher performance epoxy resins (Warrior et al. 2003). Vinyl esters shrink less during cure and outperform polyesters in chemically corrosive environments such as chemical tanks and in structural laminates requiring a high degree of moisture resistance such as boat hulls and decks.

For advanced composite matrices, the most common thermosets are epoxies, phenolics, cyanate esters (CEs), bismaleimides (BMIs) and polyimides. Epoxy matrices contribute to the strength, durability and chemical resistance of the composites. They offer increased modulus, strain to failure and high performance at elevated temperatures (Warrior et al. 2003). Epoxies come in liquid, solid and semi-solid forms and typically cure by reaction with amines or anhydrides. Most commercial epoxies have a chemical structure based on diglycidyl ether of bisphenol A and phenolic novolacs. Many aerospace applications use amine cured, multifunctional epoxies that require cure at elevated temperatures. In order to counteract their brittleness, some toughening agents

such as thermoplastics and reactive rubber particules are added (Dawson et al. 2006).

Fibers can be either amorphous or polycrystalline. Polymer aramids, glass, carbon, boron, aluminum oxide and silicon carbide are the most commonly used fiber materials. Carbon, glass, aramid fibers are the most commonly used fiber types with PMCs. Carbon is a high performance fiber material used in advanced PMCs due to their high modulus and strenght, durability in moisture, solvents, acid and bases. Carbon fibers retain their high tensile modulus and strenght at elevated temperatures. Longitudinal tensile strength and tensile modulus of aramid fibers are higher than the other polymeric fiber materials, however they are weak in compression (Hull and Clyne 1996).

The most common reinforcement for polymer matrix composites is glass fiber. Glass fibers are the oldest and the most common reinforcement used in aerospace applications to replace heavy metal parts. Glass weighs more than carbon and its impact resistance is higher than the carbon. Properties and performance of glass fibers depend on the glass type, filament diameter, sizing chemistry and fiber form. For glass reinforcement used in composites, the sizing usually contains a coupling agent to bridge the fiber surface with resin matrix used in the composite. Properties of glass fibers are determined by the fiber manufacturing process, the ingredients and coatings used in the process. Silica sand is the primary raw ingredient, and composes more than 50 percent of the glass fiber weight. Metal oxides and other ingredients can be added to the silica, and processing methods can be varied to customize the fibers (Jang et al. 1994).

Glass filaments are supplied in bundles called strands. A strand is a collection of continuous glass filaments. Yarns are the collections of strands that are twisted together. Most glass fibers are based on silica ( $\text{SiO}_2$ ), with additions of oxides of calcium, boron, sodium, iron and aluminium (Hull et al. 1996). The compositions of the most commonly used glass fibers are tabulated in Table 2.1.

Table 2.1. Glass fibre compositions  
(Source:Hull et al. 1996)

	<b>E-glass</b>	<b>C-glass</b>	<b>S-glass</b>
<b>Composition (%)</b>			
SiO <sub>2</sub>	52.4	64.4	64.4
Al <sub>2</sub> O <sub>3</sub> + Fe <sub>2</sub> O <sub>3</sub>	14.4	4.1	25.0
CaO	17.2	13.4	-
MgO	4.6	3.3	10.3
Na <sub>2</sub> O + K <sub>2</sub> O	0.8	9.6	0.3
B <sub>2</sub> O <sub>3</sub>	10.6	4.7	-
BaO	-	0.9	-

Chemical composition of E-glass (electrical glass) makes it an excellent electrical insulator, and E-glass fiber is used in the applications in which radio signal transparency is desired, such as aircraft radomes, antennae and computer circuit boards. It is also the most economical glass fiber for composites, while they offer sufficient strength in most applications (Dawson et al. 2006). High-strength glass (S-glass) was first developed for military applications in the 1960s. S-glass is more expensive than E-glass but has a higher strength, Young's Modulus and temperature resistance (Hull et al. 1996). Some properties of glass fibers are given in Table 2.2. Corrosion-resistant glass (C-glass) loses much less of its weight when exposed to the acid solutions than does E-glass. They are preferred for their high resistance against corrosion (ASM International 1987).

Table 2.2. Glass fiber properties  
(Source: Hull et al. 1996)

Properties	E-glass	C-glass	S-glass
Density, $\rho$ (g cm <sup>-3</sup> )	2.6	2.49	2.48
Thermal Conductivity, K (W m <sup>-1</sup> K <sup>-1</sup> )	13	13	13
Thermal expansivity, $\alpha$ (10 <sup>-6</sup> K <sup>-1</sup> )	4.9	7.2	5.6
Tensile strength, $\sigma$ (GPa)	3.45	3.30	4.60
Young's Modulus, E (GPa)	76	69	85.5
T <sub>max</sub> (°C)	550	600	650

## 2.2. Mechanical Behaviour of Polymer Matrix Composites

Fibre reinforced plastics are widely used in different industries, including aircraft and wind energy industries because of the specific benefits of these materials. These benefits are (among others) the high stiffness to weight ratios and the high strength to weight ratios. Especially, the wind energy industry uses glass fibre reinforced plastics for the reason that the glass fibres are relatively light, cheap and offer a great flexibility (Yang et al. 2000, Biob et al 1997).

There are many variables to consider when designing a PMC, such as geometry of the reinforcement and the nature of the interphase (Callister 2000). The interphase of PMCs is the region in which loads are transmitted between the reinforcement and the matrix. The extent of interaction between the reinforcement and the matrix is a design variable, and it may vary from strong chemical bonding to weak frictional forces (Jang 1994). Generally, a strong interfacial bond makes the PMC more rigid, but brittle. A weak bond decreases stiffness but enhances toughness. If the interfacial bond is not as strong as the matrix, debonding can occur at the interphase under certain loading conditions (Shalin 1995).

The directional characteristic of PMC gained by using continuous fibers is called isotropy. PMCs are strongest when loaded parallel to the direction of the fibers and weakest when loaded perpendicular to the fibers. When discontinuous fibers or

particules are used for reinforcement, the properties tend to be more isotropic because these reinforcements tend to be randomly oriented (Jang 1994). In an advanced composite, the toughness is complex function of the matrix, fiber, and interphase.

The fiber-matrix interfacial adhesion plays an important role in determining mechanical properties of polymer composites. Composites gain better properties such as interlaminar shear strength, delamination resistance, fatigue and corrosion resistance with a better interfacial bond. Since the interface is the most highly stressed region of a composite material, several attempts have been made to lower these stress concentrations by placing either a material with an intermediate modulus or an elastomer phase between the fiber and the matrix (Jang 1994). Delamination is one of the most critical form of the damage in PMC structures. The impact damage on the surface can cause dramatic reductions in strength through local delamination. The effects of preform structure on delamination properties of composite materials were investigated by Kim et al. and they reported that interlaminar fracture toughness of the knitted composites was strongly affected by the physical properties of the knitted preforms (Kim et al. 2005). A decrease in the areal density or tightness factor of the knitted preforms increases the strain energy release rate ( $G_{IC}$ ) of the composites and they concluded that tightness factor has affected on the interlaminar fracture toughness.

The interphase has a critical influence on the PMC in that it determines how the reinforcement properties are translated into the properties of the composite structure. The interactions between the fiber and the matrix resin before or during the curing are complex but important phenomena. These interactions could lead to the formation of the interphase, which most likely has different composition, microstructure and properties than the bulk resin. Interlayers of PMCs can be improved by using some binders or tackifiers. Hillermeier and Seferis reported that epoxy based spray tackifiers provide an improvement of 30% in Mode II interlaminar fracture toughness, a slight increase in the interlaminar shear strength without reducing the thermal properties of an RTM processed laminate (Hillermeier and Seferis 2001). Many studies revealed that fibers sizings play a major role in the strength, impact resistance and environmental durability of glass fiber reinforced composites. Tanoğlu et al. studied the effects of various glass fiber sizings on the mechanical behaviour of a glass/epoxy composite and concluded that compatible sized fibers showed higher strength values, while the unsized ones exhibited greater frictional sliding (Tanoğlu et al. 2001).

Fatigue resistance is the main advantage of PMCs over metals; however, the traditional models for analyzing fatigue of metals can not apply to PMCs. The initial imperfections in PMCs such as delamination, matrix cracking, fiber debonding, voids, etc. can be much more larger than corresponding imperfections in conventional metals such as cracks. The growth of damage in metals is much more rapid and hence dangerous than in composites (Jones 1975).

Failure of PMCs often results from gradual weakening caused by the accumulation of dispersed damages, instead of by the propagation of a single crack. On completion of the thermal cycling, the crack resistance of glass fiber reinforced PMCs is higher in the specimens reinforced with continuous fibers. The effect of fibre surface treatment is noticeable on crack resistance glass fibre reinforced PMCs in the initial state and after thermal cycling (Shalin 1995).

### **2.3. Non-Crimp Fabric Reinforced Composites**

Textile technologies such as weaving, stitching, braiding, and knitting are being employed to fabricate advanced composites with conformability, quality and integrated mechanical properties. One of the objectives of using textile reinforcement is to take advantage of through the thickness arrangement of fibers to enhance interlaminar strength and toughness, compressive strength, as well as compression after impact strength. Reinforcing fibers in the thickness direction also contribute to stiffness and strength in that direction (Jang 2000).

Table 2.3 tabulates the descriptions for textile manufacturing techniques. The internal geometry of a textile reinforcement is an important factor for the reinforcement performance during composite manufacturing and in service life of the composite material. For the former, impregnation of the reinforcement is governed by the size, distribution and connectivity of pores. Load transfer from the matrix to the reinforcement is governed by the fibre orientation, which plays a great role in the composite stiffness (Verpoest et al. 2005).

Table 2.3. Description of advanced textile manufacturing techniques

(Source:Tong 2002)

<b>Textile Process</b>	<b>Preform Style</b>	<b>Fibre Orientation</b>	<b>Productivity /setup</b>
<b>Stitching (general)</b>	Complex preforms possible by combining structures	Dependant upon basic fabric being stitched	High productivity/ short set up time
<b>3D Weaving</b>	Flat fabrics, simple profiles, integral stiffened structures & integral sandwich structures	Wide range of through-thickness architecture possible but in-plane fibers generally limited to 0/90 directions	High productivity/ long setup time
<b>3D Braiding</b>	Open and closed profiles	0 degree fibers. Braiding fibers between 0-80 degrees. 90 degree fibers possible	Medium productivity/ long setup time
<b>Knitting (Warp and weft)</b>	Flat fabrics, integral sandwich structures & very complex preforms	Highly looped fibres in meshlike structure	Medium productivity/ long setup time
<b>Knitting (Non-crimp)</b>	Flat fabrics	Multi-axial in-plane orientation 0/90/+45/-45.	High productivity/ long setup time

One of the main disadvantage of fibre reinforced plastics is complex when compared to metallic structures, because many different unidirectional layers have to be processed manually in a mold. One possibility to circumvent this is the use of weaves, another one the use of non-crimp fibers (NCFs). NCFs consist of several layers, stitched together by a stitching yarn as shown in Figure 2.4. Each layer is made up of tows of fibers placed side by side. The benefit of NCFs is that their fibres are not crimped as compared to weaves and one macroscopic layer (which consists of different sublayers) can be processed instead of several sublayers (Adden et al. 2006, Kong et al. 2004). Figure 2.5 illustrates a schematic of a woven fabric cross section. When a load is applied to a woven fabric, stress concentration occurs at every point where one fiber bundle passes over or under another. This causes stress complication locally in the weaker matrix. Laminates made of NCFs show higher compressive strength than woven fabric composites due to the less waviness. NCF composites have higher fiber volume fractions and hence higher strength, since they do not have resin pockets unlike the woven fabrics (Figures 2.5 and 2.6).

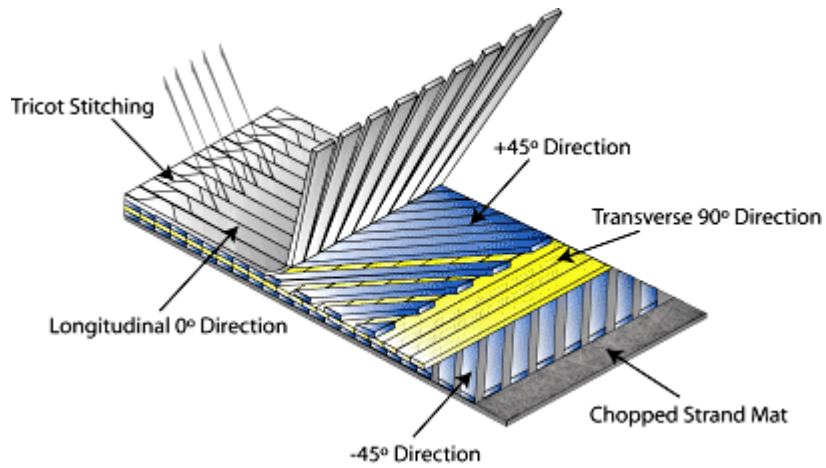


Figure 2.4. Schematic illustration of NCFs  
(Source:WEB\_2 2006)

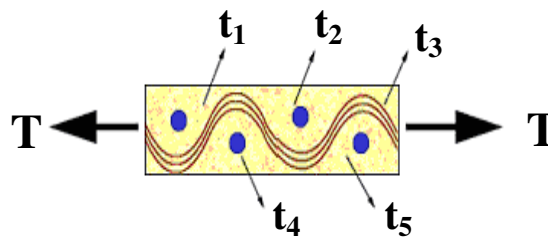


Figure 2.5. Resin pockets in a composite manufactured with woven fabrics  
(Source:WEB\_2 2006)

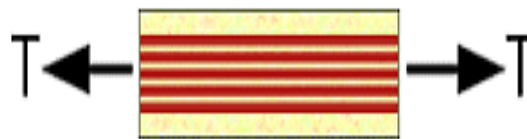


Figure 2.6. Laminate prepared with NCFs  
(Source:WEB\_2 2006)

The increasing desire of industry to exploit the performance benefits of composites is driving the search for cost reductions of their manufacturing process. The high cost of the raw materials must be offset by reduced processing and assembly costs for composites to continue to replace metals in cost sensitive applications. Non-crimp

fabrics are promising textile form, widely considered for use in this context (Bibo et al 1997). NCFs offer numerous processing advantages, but they have been shown to result in laminates with in-plane mechanical properties that are lower than equivalent laminates made from unidirectional preregs. Damage and its effect on critical properties such as compression after impact strength have been identified as key issues (Bibo et al 1997).

Yang et al. studied the mechanical properties and failure mechanisms of a glass fabric/ epoxy composite and used unstitched plain weave and biaxial non-crimp fabrics for comparison. They reported that the compressive strength of non-crimp laminate samples was about 15% higher than that for the woven fabric composites because of the waviness in woven fabric composites. Compression failure mechanism of laminate composites was observed as shear failure of fibers across the specimen thickness. For woven fabric composites, delamination followed by microbuckling and global buckling was the failure mechanism, while the non crimp fabric composites appeared to fail via kinking followed by fiber buckling (Yang et al. 2000).

The other main issue to be addressed with stitching is the improvement in resistance against delamination. Impact damage mechanism in a laminate is a combination of matrix cracking, surface buckling, delamination, fiber shear out and fiber fracture (Shyr and Pan 2003). NCF composites show definite improvements in damage tolerance which are not necessarily attributed through the thickness reinforcement provided by the stitching (Drapier et al. 1999). Damage characteristics and failure strengths of composite laminates were investigated by Shyr and Pan and composites were fabricated by using a polyester matrix with three different fabrics i.e.; non crimp fabric, woven fabric and non woven mat (Shyr and Pan 2003). They concluded that impact energy absorption of laminates varies with the fabric structure and the non-crimp fabric was the most appropriate selection for composite laminates because of their increasing impact resistance property.

## CHAPTER 3

### NANOPARICULATE FILLED COMPOSITES

#### 3.1. Layered Silicates

Smectite clay is the most commonly used clay type to obtain nanoparticles suitable for nanocomposite production. Clays utilized in preparing polymer-clay nanocomposites belong to the 2:1 layered structure type. As being a member of the 2:1 family, montmorillonite (MMT) is a layered aluminosilicate in the smectite family of clays (Qutubuddin et al. 2001, Hackmann and Hollaway 2006).

Smectic clays or phyllosilicates show relatively weak bonding between the layers comprised of small flakes. Each layer consists of two sheets of silica tetrahedra with an edge shared octahedral sheet of either alumina (aluminosilicates) or magnesia (magnesium silicates). Due to isomorphic substitution of alumina into the silicate layers ( $\text{Al}^{3+}$  for  $\text{Si}^{4+}$ ) or magnesium for aluminium ( $\text{Mg}^{2+}$  for  $\text{Al}^{3+}$ ), each unit cell has a negative charge between 0.5 and 1.3. These layers are held together with a layer of charge compensating cations such as  $\text{Li}^+$ ,  $\text{Na}^+$ ,  $\text{K}^+$ , and  $\text{Ca}^+$  (Qutubuddin et al. 2001). These charge compensating cations provide a route to the rich intercalation chemistry and surface modification is required to disperse clays at the nanoscale into polymers. MMT can be delaminated and dispersed into individual platelets that have thickness in the nanometer level and the other dimensions typically 70 nm to 150 nm across. The delamination of the individual layers increases the surface area to volume ratio (Hackmann and Hollaway 2006). The cation exchange capacity (CEC) of clay defines the number of exchangeable interlayer cations and is usually described as mEq/100g. CEC values range from 60 to 120 for smectic clays (Ajayan et al. 2003). A typical structure of 2:1 layered silicate is shown in Figure 3.1.

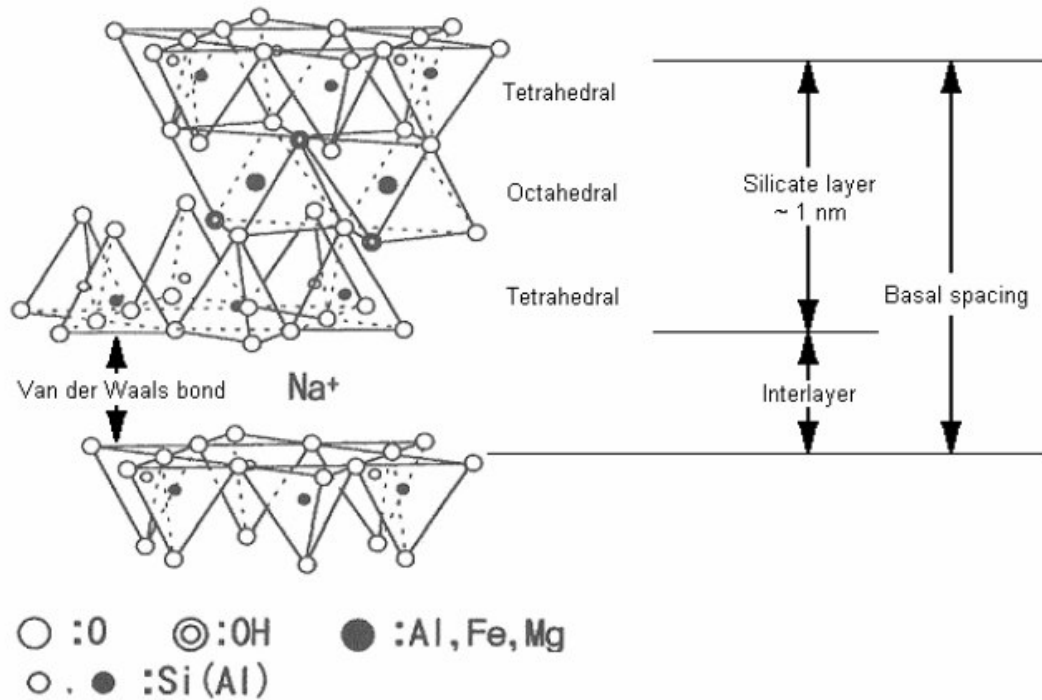


Figure 3.1. The structure of 2:1 layered silicates

(Source: Meneghetti et al. 2005)

### 3.2. Modification of Layered Silicates

MMT particules without individual separation are often referred to as tactoids. When tactoids are partially separated in a polymer, they are referred to be intercalated. When thoroughly separated, individual plalets are said to be exfoliated (Dawson et al. 2006). Silicate clays are inherently hydrophilic, but polymers tend to be hydrophobic. These presents an interesting challange in terms of being able to disperse the silicate layers in a polymer (Ajayan et al. 2003). Pristine layered silicates usually contain hydrated  $\text{Na}^+$  or  $\text{K}^+$  ions. Ion exchange reactions with cationic surfactants, including primary, tertiary and quaternary ammonium ions, render the normally hydrophilic silicate surface organophilic, making the intercalation of many engineering polymers possible (Giannelis 1998). Generally the surface of the clay needs to be modified to improve the wettability and dispersibility of hydrophilic clay. This modification is also known as compatibilisation. Because of the isomorphic substitution by low covalent atoms, sheet backbone produces some negative charges balanced by some cations in the gallery. These cations can be easily exchanged with surfactants including alkyl

ammonium cations (Chen et al. 2003). The role of the alkylammonium cations in the organosilicates is to lower the surface energy of the inorganic component and improve the wetting characteristics with the polymer. Additionally, the alkylammonium cations can provide functional groups that can react with the polymer or initiate a polymerization of monomers to improve the strength of the interface between the inorganic component and the polymer (Giannelis et al. 1998)

Not only the chemical product used as treating agent, but the way in which this substitution is performed has effect on the formation of particular nanocomposite. The laboratory technique commonly used to introduce alkylammonium ions in the interlayer is an ion exchange reaction that promotes the formation of the desired ion dissolving either the related amine together with a strong acid (Kawasumi et al. 1998) or a salt which has long alkyl chain cation linked to counter ions as chloride or bromide into hot water (about 80°C). Such solution has to be poured into the blend of MMT previously dispersed into hot water. A stirring with a homogenizer is required to yield white precipitates which have to be collected, washed and eventually dried. Surface treatment of hydrophilic clay is schematically illustrated in Figure 3.2.

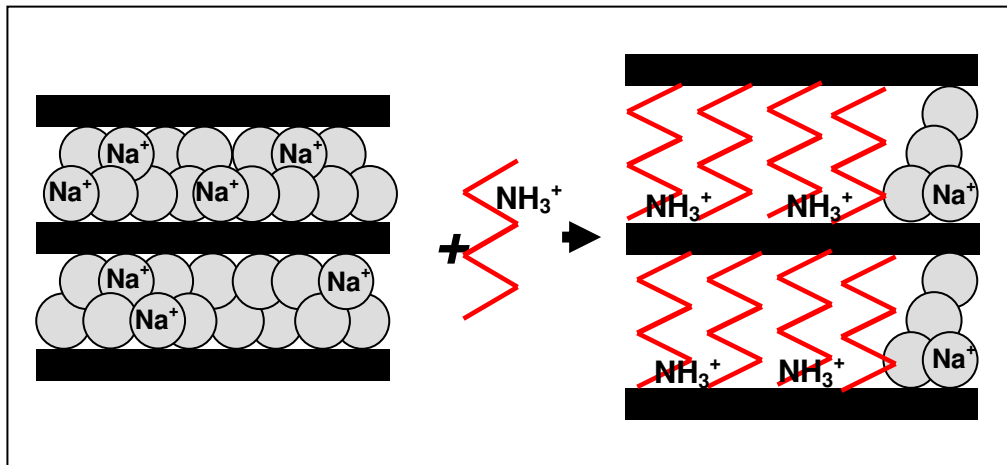


Figure 3.2. Schematic representation of clay surface treatment

The surface treatment procedure is not only used to render the clay an organoclay, but also used to improve the wetting characteristic with a polar polymer. Surface treatment also increases the interlayer distance. Indeed surface treated clay is used even in case of polar polymers in which the modification of clay polarity is not fundamental for the nanocomposite production. Clearly, as the amount of carbon atoms

in the tail of the ammonium ion increases, the clay becomes more organophilic; the introduction of a longer organic molecule in the clay structure helps to increase the interlayer distance as well. Hexadecyl-trimethyl-ammonium ion or dioctadecyl-dimethyl-ammonium ion are typical surfactants used for this purpose (Ajayan et al. 2003).

### **3.3. Layered Silicate/ Polymer Nanocomposites**

Conventional particulate filled polymer composites are widely used in diverse applications, such as construction, transportation, electronics, and consumer products. Composites offer improved properties, including higher strength and stiffness as compared to the nonfilled polymers (Qutubuddin et al. 2001). The properties of polymer composites are greatly affected by the dimension and microstructure of the dispersed phase. Nanocomposites possess special properties due to large interfacial area per unit volume or weight of the dispersed phase (Ajayan et al. 2003). Clay layers dispersed at the nanoscale in a polymer matrix act as a reinforcing phase to form polymer-clay nanocomposites, an important class of organic-inorganic nanocomposites (Chen et al. 2003).

There are several different methods to synthesize polymer-clay nanocomposites; melt intercalation, solution and in-situ polymerization.

#### **3.3.1. Melt Intercalation**

A thermoplastic polymer is mechanically mixed with an organophilic clay at elevated temperatures. The polymer chains are then intercalated between the individual silicate layers of the clay. The proposed driving force of this mechanism is the enthalpic contribution of the polymer/organoclay interactions. This method is becoming increasingly popular since the resulting thermoplastic nanocomposites may be processed by conventional methods such as extrusion and injection molding (Ahmadi et al. 2004).

### **3.3.2. Solution Method**

In the solution method, the organoclay, as well as the polymer, are dissolved in a polar organic solvent. The entropy gained by the desorption of solvent molecules allows the polymer chains to diffuse between the clay layers, compensating for their decrease in conformational entropy. After evaporation of the solvent, an intercalated nanocomposite results. This strategy can be used to synthesize epoxy-clay nanocomposites but the large amount of solvent required is a major disadvantage (Ahmadi et al. 2004)

### **3.3.3. In-situ Polymerization**

The in-situ polymerization approach was first developed by Toyota group to develop Nylon-6 nanocomposites from caprolactam monomer. It has been applied to several other systems, including epoxies and styrene. This technique was found to be most effective one for a thermoset polymer matrix nanocomposite (Nigam et al. 2004). It is similar to the solution method except that the role of the solvent is replaced by a polar monomer solution. Nanoscale particles are dispersed in the monomer or monomer solution, and the resulting mixture is polymerized by standard polymerization methods (Qutubuddin et al. 2005). The polymerization is believed to be the indirect driving force of the exfoliation. The clay, due to its high surface energy, attracts polar monomer molecules in the clay galleries until equilibrium is reached. The polymerization reactions occurring between the layers lower the polarity of the intercalated molecules and displace the equilibrium. This allows new polar species to diffuse between the layers and progressively exfoliate the clay. Therefore, the nature of the curing agent as well as the curing conditions is expected to play a role in the exfoliation process (Kornmann et al. 2001).

## **3.4. Morphology of Layered Silicate/Polymer Nanocomposites**

The specific characteristics of nanocomposites can be effective only if the nanoparticles are well dispersed in a nanoscale level in the surrounding polymer

composites (Lin et al. 2005). Complete dispersion or exfoliation of clay tactoids in a monomer or polymer matrix may involve three steps similar to the dispersion of powders in liquids. The first step is wetting the surface of clay tactoids by monomer or polymer molecules. The second step is intercalation or infiltration of the monomer or polymer into the clay galleries, and the third step is exfoliation of clay layers. The first and second steps are determined by thermodynamics, while the third step is controlled by mechanical and reaction driving forces (Qutubuddin et al. 2001). The dispersion of clay tactoids in a polymer matrix can result in the formation of three types of morphology, as shown in Figure 3.3.

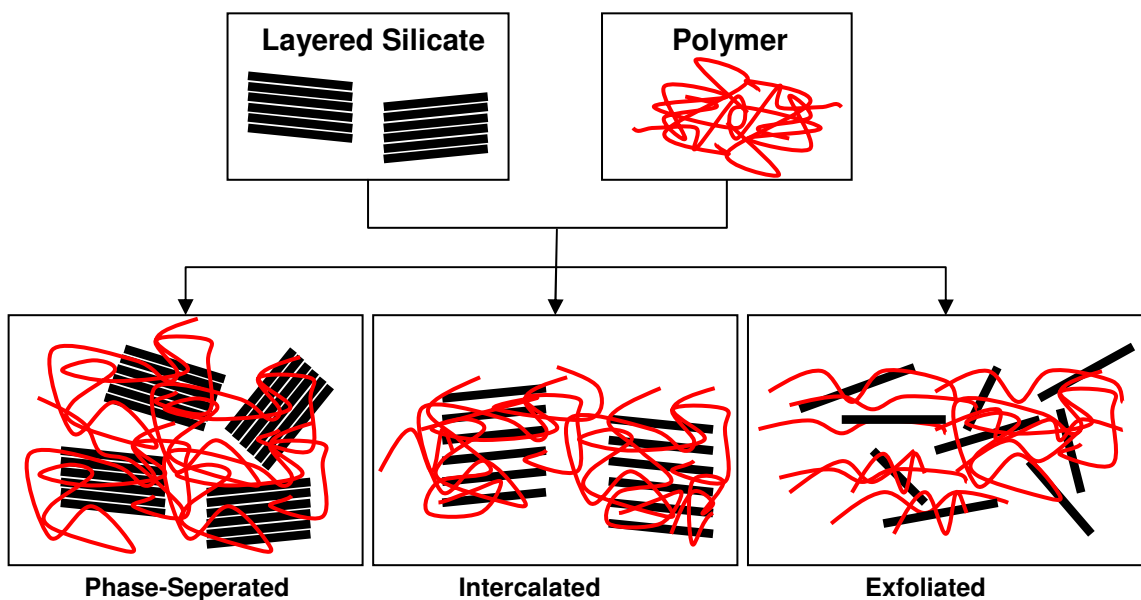


Figure 3.3. Morphologies of polymer/clay nanocomposites

The first type is a conventional composite that contains clay tactoids with the nanolayers aggregated in unintercalated face to face form. In this case, clay tactoids are dispersed simply as a segregated phase, resulting in poor mechanical properties of the composite. The second type is intercalated polymer/clay nanocomposite which is formed by the infiltration of one or more molecular layers of polymer into the clay host galleries (Qutubuddin et al. 2001). In an intercalated nanocomposite, the insertion of polymer into the clay structure occurs in a crystallographically regular fashion and typically few molecular layers of polymer occupy the gallery region (Ranta et al. 2003, Luo et al 2003). The last type is exfoliated polymer/clay nanocomposites, characterized

by low clay content, a monolithic structure, and a separation between clay layers that depends on the polymer content of the composite. Exfoliation is particularly desirable for improving specific properties that are affected by the degree of dispersion and resulting interfacial area between polymer and clay nanolayers. In an exfoliated nanocomposite, the individual (about 1 nm thick) clay layers are dispersed in a continuous polymer matrix and segregated from one another by average distances that depend on clay loading. Hence, an exfoliated nanocomposite has a monolithic structure with properties related to those of the starting polymer. The greatest property enhancements are observed for exfoliated or delaminated epoxy/clay nanocomposites (Ranta et al. 2003)

The exfoliation of the clay can occur only at the earlier curing stage before the gel point of thermosetting polymer is reached. There is a curing competition between intragallery and extragallery epoxy. If the intragallery cure reaction is faster than the extragallery, the intragallery epoxy can cure fully before the extragallery epoxy reaches its gelpoint. As a result, the curing heat produced is enough to overcome the attractive forces between the silicate layers, so the clay will be exfoliated. In contrast, if the extragallery epoxy cures faster, it will gel before the intragallery epoxy produces enough curing heat to drive the clay to exfoliate. Consequently, the clay can not reach total exfoliation. Therefore, the curing speed of intragallery epoxy relative to that of extragallery epoxy is an important factor influencing the exfoliation of clay (Jiankin et al. 2000).

### **3.5. Properties of Nanocomposites**

Nanofillers have for many years had a high significance in the plastics industry. Nanofillers are basically understood to be additives in solid form, which differ from the polymer matrix in terms of their composition and structure. They generally comprise inorganic materials, more rarely organic materials. Inactive fillers or extenders raise the quantity and lower the prices, while active fillers bring about targeted improvements in certain mechanical or physical properties. The activity of active fillers may have a variety of causes, such as the formation of a chemical bond (e.g., cross linking by carbon black in elastomers) or filling of a certain volume, disruption of the

conformational position of a polymer matrix, the immobilization of adjacent molecule groups and the possible orientation of the polymer material (Ranta et al. 2003).

Nanocomposites usually exhibit better physical and mechanical properties than their micro counterparts because of their unique phase morphology and improved interfacial properties (Jiankun et al. 2000). Carbon nanotubes and ceramic nanoparticles are used as highly functional fillers or additives in polymer products of interest to composite manufacturers. Introduction of these materials can result in the improvement of the polymer's mechanical properties in molded parts and coatings on a wide variety of fronts, including increased part strength, ductility and dimensional stability as well as resistance to damage by abrasion exposure to caustic chemicals and extreme heat. Carbon nanotubes is relatively new materials (Dawson et al. 2006) and these nanosized, near perfect tubes were first noticed and fully characterized in 1991 by Sumio Iijima of NEC Corporation in Japan. He was investigating the surface of carbon electrodes used in an electric discharge apparatus that had been used to make fullerenes (Ajayan et al. 2003).

The most common 2D fillers are layered silicates because of their layered structures. Increasing the interlayer spacing of clay plaques is possible by surface modification due to the weak bonds between the layers which eases the dispersion properties of clays in polymers. Most of the work carried out in the polymer nanotechnology area is concentrated on the improvement of thermal, mechanical, optical, barrier properties of thermosetting and thermoplastic polymer systems. Intercalation and exfoliation behaviour of organoclays in epoxy resin has been studied through XRD and TEM analysis by many authors (Jiankun et al. 2000, Chen and Yang 2001, Nigam et al. 2004, Ratna et al. 2003). They all have found that the organoclays were easily intercalated by epoxy oligomer to form a stable epoxy/clay intercalated hybrid and the exfoliation ability of organoclays was basically determined by the nature of the clays and the curing agent used. It was reported that, increasing the cure temperature increases the interlayer spacing of silicate layers (Dean et al. 2005). Kaya et al. synthesised epoxy/silicate nanocomposites with both modified (OMMT) and unmodified silicates (MMT). As shown in Figures 3.4. a and b, in OMMT/epoxy nanocomposites, organosilicate platelets are better dispersed in epoxy as compared to those MMT/epoxy nanocomposites (Kaya et al. 2006).

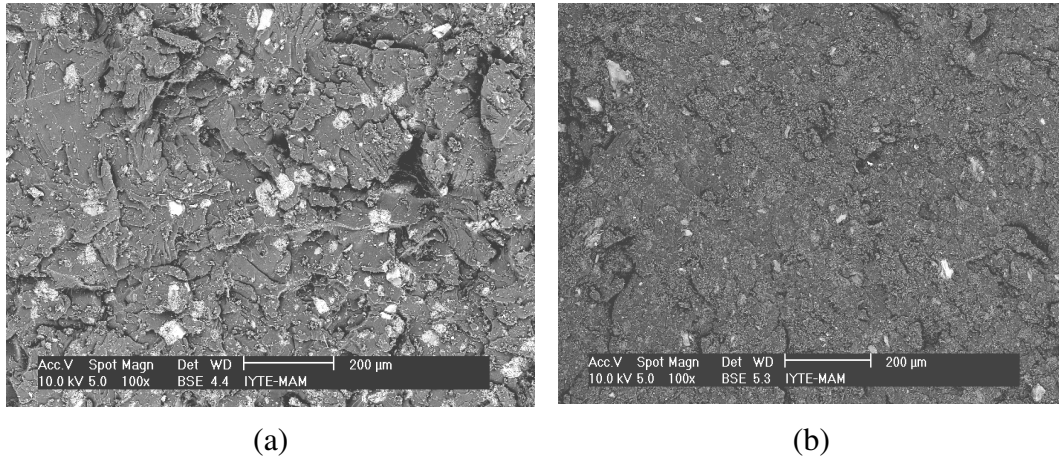


Figure 3.4. SEM micrographs of fracture surfaces of (a) epoxy/ 3 wt. % MMT (b) epoxy/ 3 wt. % OMMT nanocomposites ( Source: Kaya et al. 2006)

Investigations on the mechanical properties of layered silicate/epoxy nanocomposites showed that addition of layered silicates has some influence on the tensile strength and modulus, elongation at break, flexural strength and modulus, fracture toughness (Kaya et al. 2006). As shown in Figures 3.5. a and b, tensile modulus increased with the addition of both MMT and OMMT, but addition of MMT decreased the tensile strength of nanocomposites, while it remains constant with OMMT additions. The strain at break values decreased with increasing silicate content for both nanocomposites containing MMT and OMMT. According to the authors, the decrease in tensile strength with the addition of MMT was related to the agglomeration formed due to the inhomogeneous dispersion of silicates. It was also reported by the same authors that flexural modulus of nanocomposites increased with the addition of both MMT and OMMT silicates, while the flexural strength values decreased. This reduction was related to the measured void content, with increasing silicate loading.

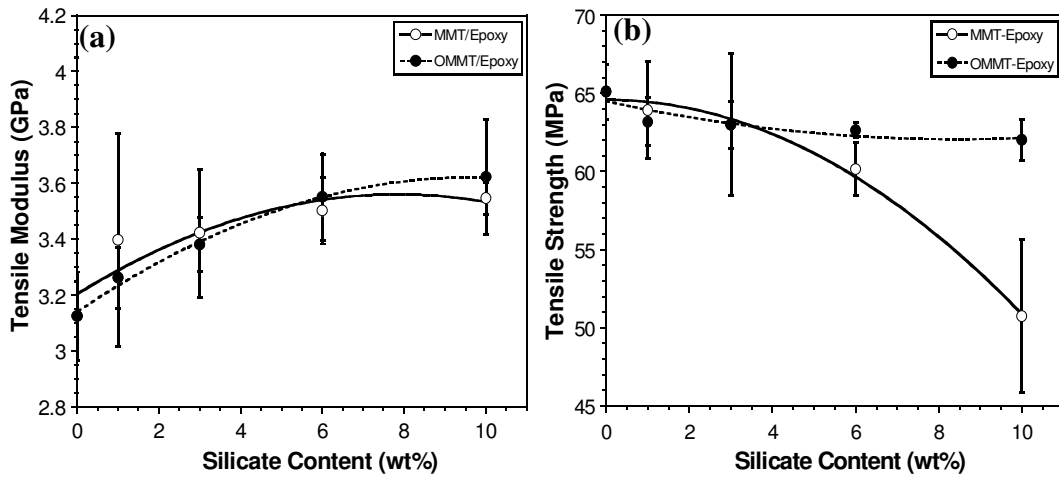


Figure 3.5. (a) Tensile modulus and (b) tensile strength of silicate/epoxy nanocomposites (Source: Kaya et al. 2006)

Nigam et al. modified the montmorillonite clay with octadecylamine surfactant and made it organophilic (Nigam et al. 2004). Mechanical properties of epoxy/clay nanocomposites attained maximum value at 6 wt. % loading of exfoliated clay as shown in Figures 3.6, 3.7 and 3.8. They reported that the decrease in the mechanical properties beyond that level was due to inhomogeneous filler dispersion. An increase in the clay concentration from 0 to 6 wt. % lead to 100 % increase in the tensile modulus, 20% increase in the ultimate tensile strength and 80 % decrease in the elongation at break values. They also reported that the organoclay composite showed higher mechanical properties than the composites prepared with inorganic ones.

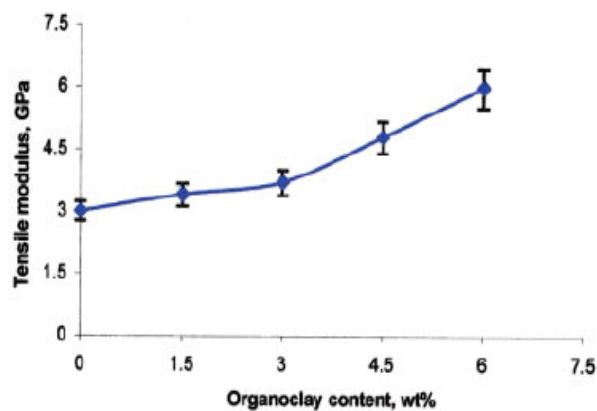


Figure 3.6. Tensile modulus of epoxy/clay nanocomposites as a function of clay concentrations (Source: Nigam et al. 2004)

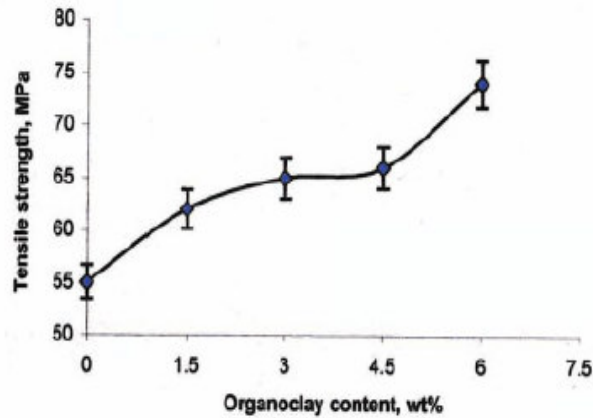


Figure 3.7. Tensile strength of epoxy/clay nanocomposites as a function of clay concentrations (Source: Nigam et al. 2004)

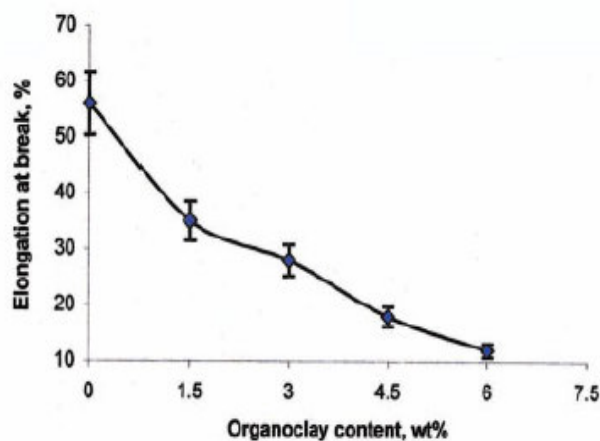


Figure 3.8. Elongation at break of epoxy/clay nanocomposites as a function of clay concentrations (Source: Nigam et al. 2004)

The effect of clay loading on the fracture toughness of epoxy was investigated by Liu et al. (Liu et al. 2005). The fracture toughness of nanocomposites was measured using the single edge notch bending technique. It was observed that the critical stress intensity factor ( $K_{IC}$ ) and critical strain energy release rate ( $G_{IC}$ ) increased by 2.2 and 5.8 times, respectively, over those of pristine resin properties at 4.5 phr (about 3% weight) clay loading. They also synthesized organoclay-modified high performance epoxy nanocomposites with both direct mixing method (DMM) and high pressure mixing method (HPMM). The increase in the basal spacing of organoclay was found to

be greater with DMM as observed from XRD but organoclay was aggregated in the epoxy resin because of the inhomogeneous dispersion. The extent of agglomeration increased with increasing clay loading but only small portion of the interphases between the resin and the particules were debonded (Figure 3.9). According to Liu et al. epoxy molecules were intercalated into the organoclay and had a good interface with the platelets of organoclay and these results with the formation of rigid and well-bonded agglomerates. These particules impeded the propogation of cracks.

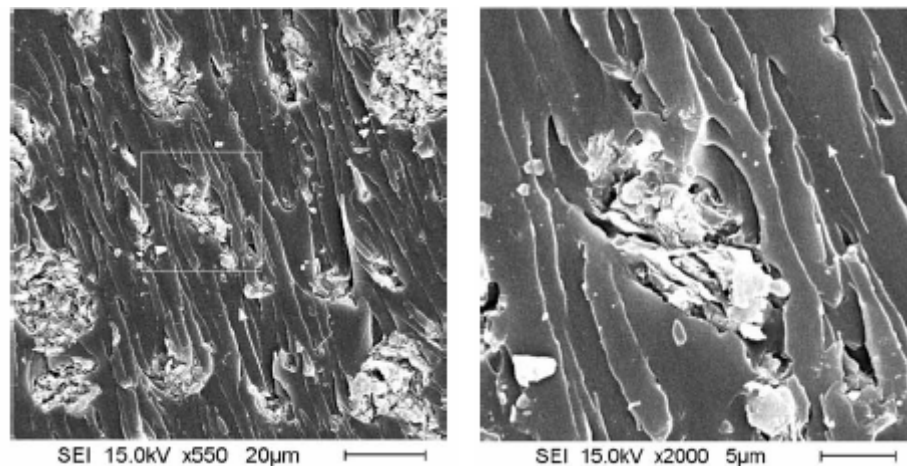


Figure 3.9. SEM micrographs of fracture surfaces of nanocomposites made with the DDM (Source: Liu et al. 2005).

Chen et al. synthesized an epoxy-montmorillonite nanocomposite and they showed that clay loading increased the glass transition temperature of the composite as shown in Figure 3.10. Besides these improved thermal properties, water resistance and optical properties of nanocomposites were positively influenced (Chen et al. 2002).

Lee et al. prepared epoxy-MMT hybrid composites without using ion exchange reaction with alkyl or aryl onium ions or by employing special coupling agents (Lee et al. 1998). They observed that DSC analysis of cured products showed clear transition points corresponding approximately to the  $T_g$  of the cured epoxy polymer.  $T_g$  of cured polymer increased by 33% with loading of 40 phr montmorillonite clay. Liu et al. synthesised epoxy/clay nanocomposite with an octadecyl amine modified montmorillonite and reported that the surface modifiers in the organoclay at high temperature might exist in the system and act as a lubricator as a result of decreased  $T_g$  of nanocomposites (Liu et al. 2005).

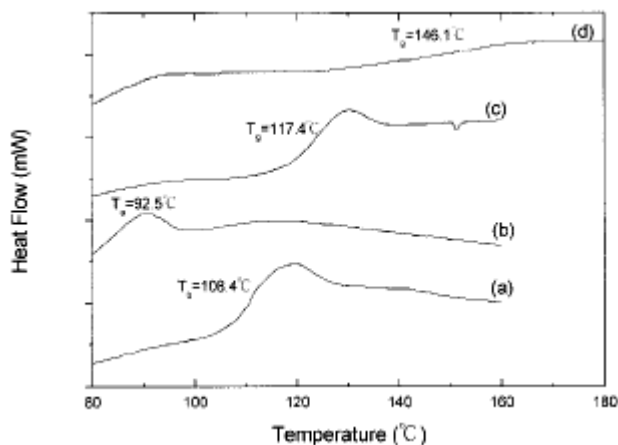


Figure 3.10. DSC thermograms of epoxy/clay nanocomposites (a) no clay addition (b) 20 phr MMT (c) 5 phr OMMT (d) 20 phr OMMT (Chen et al. 2002)

Although clays are microns in lateral size, and just 1 nm thick and when single layers are dispersed in a polymer matrix, the resulting nanocomposite is optically clear in visible light. Kaya et al. reported that optical transmission values were affected by MMT and OMMT silicate incorporation. Transmission values decreased with increasing silicate loading and nanocomposites containing OMMT silicate particles showed better transparency than those containing MMT because of the nanosized thickness of organically modified silicate layers. Clays are presumably increase the barrier properties by creating a maze or ‘tortuous path’ (Figure 3.11) that retards the progression of the gas molecules through the matrix resin. The direct benefit of the formation of such paths was clearly observed in polyimide/clay nanocomposites by improved barrier properties, with a simultaneous decrease in the thermal expansion coefficient (Ray et al. 2003). Similarly, incorporation of increasing amounts of montmorillonite particles reduced the helium gas permeability with the formation of tortuous path in silicate nanocomposites (Ogasawara et al. 2006).

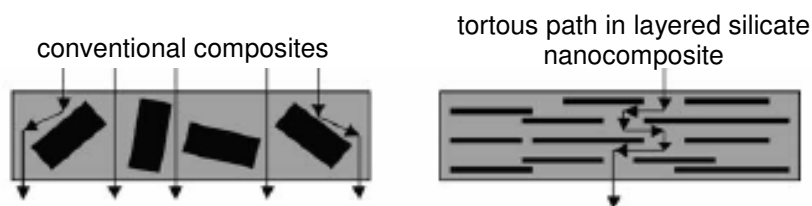


Figure 3.11. Formation of tortuous path in nanocomposites (Source: Ray et al. 2003).

The effect of the addition of nanoscaled multi-layered aluminosilicates on the barrier properties of a polymer was investigated by Thomassin et al.. The measurements on the barrier properties showed that the addition of 7 wt.% of silicate is able decreased the methanol permeability by 88% with respect to the neat polymer (Thomassin et al. 2006). The permeability reduction was also shown to depend on the specific aspect ratio of clays being used as illustrated in Figure 3.12 (Hackmann and Hollaway 2006).

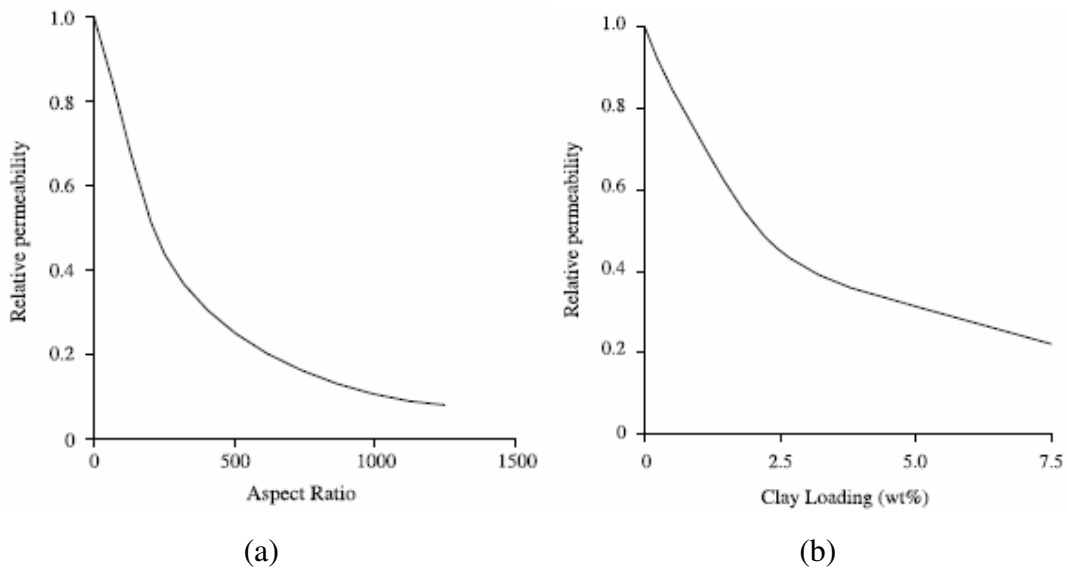


Figure 3.12. Relationship between (a) aspect ratio and relative permeability (b) clay loading and relative permeability of a clay with an aspect ratio of 250 (Source: Hackmann and Hollaway 2006).

### 3.6. Nanofiller Added Fabric Reinforced Composites

Incorporation of nano particules (clays, carbon nanotubes and etc.) in the matrix sytem of fiber reinforced composites has been studied recently. Generally, the preparation of fiber reinforced composites with nanofiller addition affected the matrix dominated properties of composites. Kornmann et al. investigated glass fiber reinforced laminates with a matrix of epoxy/layered silicate system and showed that flexural stenght of the composites is increased in laminates with the presence of the layered silicates in the matrix. They explained this increase in flexural strength with the presence of silicate layers at the surface of the glass fibers, which may improve the

interfacial properties between the matrix and the fibers (Kornmann et al. 2005). The glass fiber reinforced polymers with carbon nanotube/epoxy matrix were investigated by Gojny et al. via resin transfer molding, and they showed that tensile properties of laminates were not influenced while the matrix dominated properties such as interlaminar shear strength and fracture toughness increased (Gojny et al. 2005). The matrix dominated properties were related to the increased strength of epoxy matrix caused by the nano reinforcements and the strengthened interface between glass fibers and nanoparticules. Subramaniyan et al. studied composites with stitched unidirectional E-glass fibers and an epoxy vinyl ester resin via vacuum assisted wet lay-up method, which was developed to eliminate the problem of nanoclay being filtered by the mold constituents (Subramaniyan et al. 2006). It was observed that the addition of nanoclay increased the compressive strength of glass fiber reinforced composites for different off-axis angles as shown in Figure 3.13. The improvements or reductions in compressive strength are shown on the Figure 3.13 and set 1 and 2 indicate the specimens with a fiber volume fraction of 22 and 36 %.

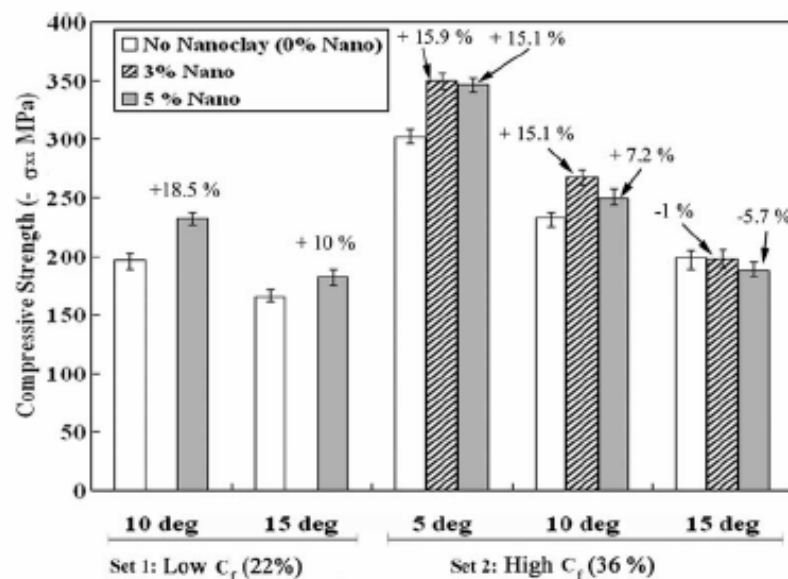


Figure 3.13. Compressive strength results of fiber reinforced composites (Source: Subramaniyan et al. 2006).

The enhancement of compressive strength with respect to clay loading reduced with increasing off-axis angles. For small off-axis angles, failure took place at the stage when the plastic strain in the matrix was small and elastic-plastic modulus of the matrix

with nanoclay was higher than that of the clear matrix. For large off-axis angles, the plastic strain in the matrix was large where the matrix with nanoclay had lower elastic-plastic modulus than that of the clear resin and this resulted with the reduction in strength. Chowdhury et al. investigated the effects of nanoclay particules on flexural and thermal properties of woven carbon fiber reinforced polymer matrix composites and found that nanoclay additon at low concentrations increased the flexural properties (Chowdhury et al. 2006). Miyagawa et al. studied the influence of biobased clay/epoxy nanocomposites as a matrix for carbon fiber composites and found that the addition of nanoclay had no effect on flexural strenght and modulus (Miyagawa et al. 2006).

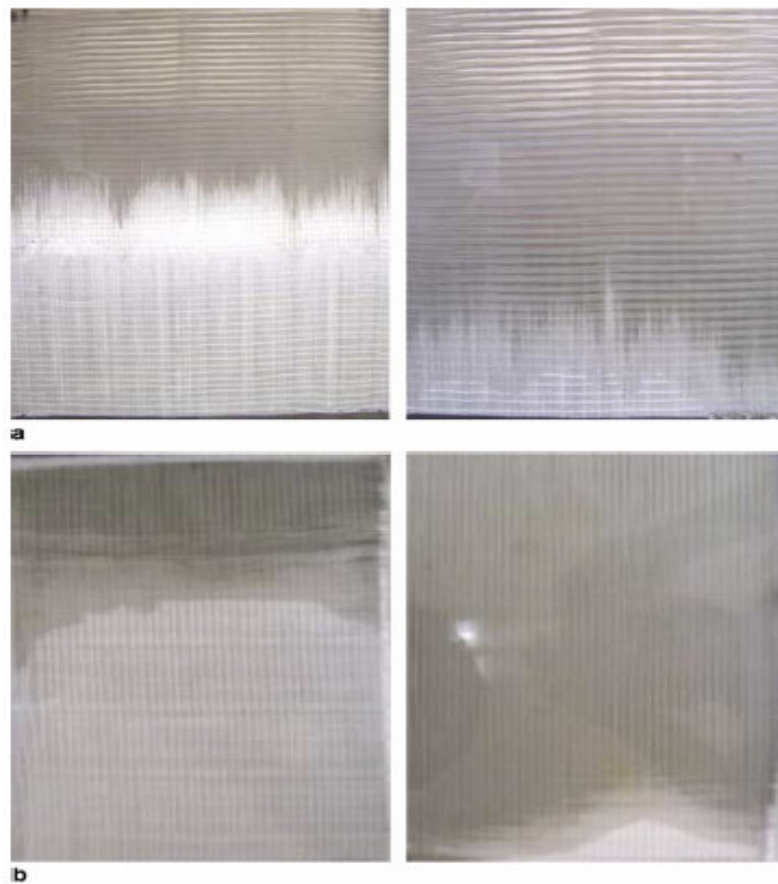


Figure 3.14. Flow patterns with different fiber directions; (a) transverse direction; (b) longitudinal direction (Source: Lin et al. 2006).

Fiber direction had effects on clay distribution in the layered silicate/glass fiber/epoxy hybrid composites when they were manufactured with vacuum assisted resin transfer molding (Lin et al 2006). They placed the unidirectional glass fibers paralel and

perpendicular to the resin flow direction and prepared laminates using vacuum assisted resin transfer molding. It was shown that mechanical properties were deviated with the direction of resin flow and location of glass fibers, and the composite properties were improved with the clay loading. When unidirectional glass fibers are placed in the transverse direction to the flow, it is easy to change the shape and position of glass fibers because of the resistance of to resin flow. This resistance leads to poor impregnation of resin and produces high void content as shown in Figure 3.14.

## CHAPTER 4

# FIBER REINFORCED POLYMER COMPOSITE MANUFACTURING METHODS

### 4.1. Hand Lay-up

The most basic fabrication method for composites is hand lay-up, which consists of laying dry plies or prepreg plies by hand onto a tool to form a laminate stack. Resin is applied to the dry plies after lay-up is complete or each ply is coated with resin (wet lay-up), before it is placed. After applying the resin to the dry plies, the wet composite is rolled by hand with a roller to distribute the resin and remove the air pockets. This procedure is repeated for each layer until the desired thickness is reached. Several curing methods are available. The most basic method is simply to allow the curing to occur at room temperature. Heat can be applied to accelerate the cure, typically with an oven. This method does not require special handling of wet fabrics. However, variances in resin viscosity cause problems in getting good wet out. To prevent the composite from sticking to the mold, a mold releasing agent is first applied to the mold (Dawson 2006, Lee 1990).

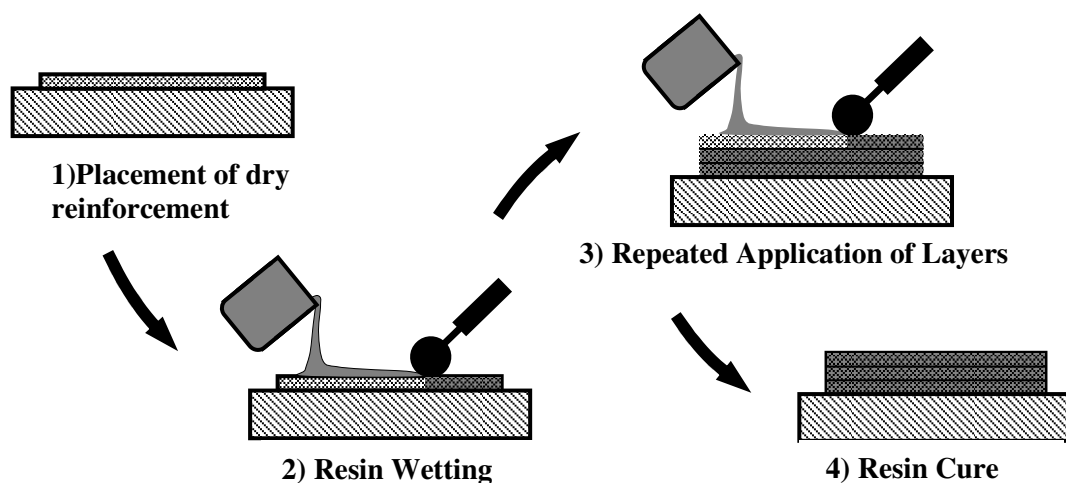


Figure 4.1. Schematic illustration of hand-lay up

The mold release can be silicone, polyvinylalcohol (PVA), fluoro-carbon or in some cases a plastic film (Lee 1990). The most popular mold releasing use fluoro-carbon in a solvent or carrier system that evaporates, leaving a thin film of fluoro-carbon material on the tool surface. Silicones are less desirable because they leave silicone residues on the cured composite surface that prevent subsequent bonding, priming or painting (ASM International Handbook 1987). For many commercial applications, a layer of catalyzed resin is applied to the mold and allowed to cure to the gel state before reinforcement is applied. This resin layer is called the gel coat and forms a protective surface layer through which fibrous reinforcement do not penetrate.

Molds can be made of almost any material that will hold its shape and they can be male or female types. Molds made of wood, plastics, composites and metals are common, since pressures are low and little strength is required. Molds for long runs are usually made of fiberglass-epoxy or metal and composite molds are especially favored because they can be formed against smooth surfaces and therefore do not require further finishing (Lee 1990). In addition, there are no corrosion problems, as there are with some metal molds. Because this technique uses one sided mold, manufactured part has one finish surface.

A laminate must be consolidated through cross linking of the resin (Karlsson et al. 1997). Many high-performance parts require both heat and high consolidation pressure to cure; therefore if they require the use of an autoclave. Autoclaves are generally expensive to buy and operate. Manufacturers equipped with autoclaves usually cure a number of parts simultaneously (Dawson et al. 2006). Successful crosslinking normally requires precise control of laminate temperature and pressure as function of time. The simplest crosslinking requirements possible are ambient conditions, i.e. room temperature and no externally applied pressure, which with some resins result in reasonably well-consolidated laminates (Karlsson et al. 1997).

With the hand-up technique, resin type is limited with the addition type crosslinking resins, since the condensation type resins require some form of pressure to avoid porous, poorly laminated structure. The resin content is often quite high and there are voids in the laminates manufactured with this method when pressure or vacuum is not used in order to compact the laminates. Also shrinkage of resin rich areas impairs the mechanical properties of composites (Lee 1990).

Due to low capital and high labor costs, wet hand lay-up is used for products manufactured in short series and where the requirements on structural and environmental properties are not excessive (Karlsson et al. 1997). Motor and sailing yachts, mine sweepers, refrigerated trucks, turbine blades, railroad containers and storage tanks are some applications of hand lay up technique.

## **4.2. Resin Transfer Molding**

RTM is a simple process and it begins with a two part, matched, closed mold which is made of metal or composite material. Dry reinforcement is placed into the mold, and the mold is closed. Resin and catalyst are metered and mixed in dispensing equipment, then pumped into the mold under low pressure through injection ports, following predesigned paths through the preform. Extremely low viscosity resin is used in RTM applications for thick parts, to permeate preforms quickly and evenly before cure (Dawson et al. 2006). Both mold and resin can be heated for particular applications if it is necessary. RTM produces parts that do not need to be autoclaved. Cure occurs within the mold, often assisted by heating if necessary (Karlsson et al. 1997). Most RTM applications use a two-part epoxy formulation. The two parts are mixed just before they are injected. Bismaleimide and polyimide resins are also available in RTM formulations.

The complexity of each stage will depend on the mold shape, preform architecture and the design of the mold. The mold shape and preform architecture would be dictated primarily by the part design. The design details of the mold, such as gate and vent locations, runners for resin and similar factors, can be adjusted for the ease of manufacturing.

The capability of rapid manufacture of large, complex, high-performance structures is one of the most important advantage of RTM. The low pressure of the process allows very large components to be manufactured. The ability to preplace the reinforcement where desired, and have it remain in that location, gives increased design flexibility and a subsequent optimized structure. RTM is a closed mold process, which has advantages over open-mold processes, including low vapor emissions. The resulting components have both inner and outer surfaces that are dimensionally controlled. Beside these advantages, RTM has still problems with filling large parts with high fiber content

at low injection pressures. Preform fabrication for high volume components also currently has limitations (ASM International Handbook 1987).

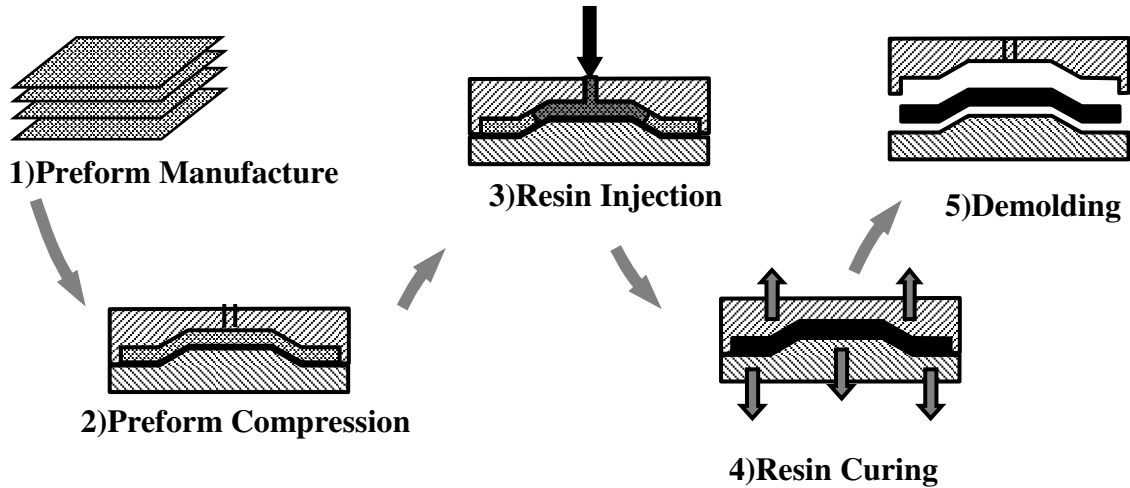


Figure 4.2. Schematic illustration of RTM

RTM technology is increasingly used in automotive applications include bumper beams, spare tire coners, crossbars, instrument panel support, pick-up truck bed liners, exterior doors, quarte panels and roofs (Gutowski 1997).

### 4.3. Vacuum Assisted Resin Transfer Molding

Vacuum-assisted resin transfer moulding (VARTM) is a liquid moulding technology used to manufacture composite components. It is the process of infusing a resin into a dry preform using vacuum assistance. The injection and outlet ports are positioned to ensure that the resin flows and fills the preform. The preform is typically vacuum bagged against a single sided tool (Crothers et al. 2002).

The VARTM process involves the following steps:

1. Mold preparation and fabric lay up.
2. Sealing the mold and running vacuum.
3. Resin preparation and degassing.
4. Resin impregnation.
5. Post cure of fabricated panels.

In the VARTM process, fiber reinforcements are placed in a one-sided mold, and a cover (rigid or flexible) is placed over the top to form a vacuum tight seal. A peel ply material, which are generally made up of Teflon treated nylons, is placed between the fiber reinforcements and the processing constituents to separate them from the part. The resin typically enters the structure through strategically placed ports. It is drawn by vacuum through the reinforcements by means of a series of designed in channels that facilitate wet out of the fibers. Fiber content in the finished part can be as high as 70 percent. Current applications include marine, ground transportation and infrastructure parts.

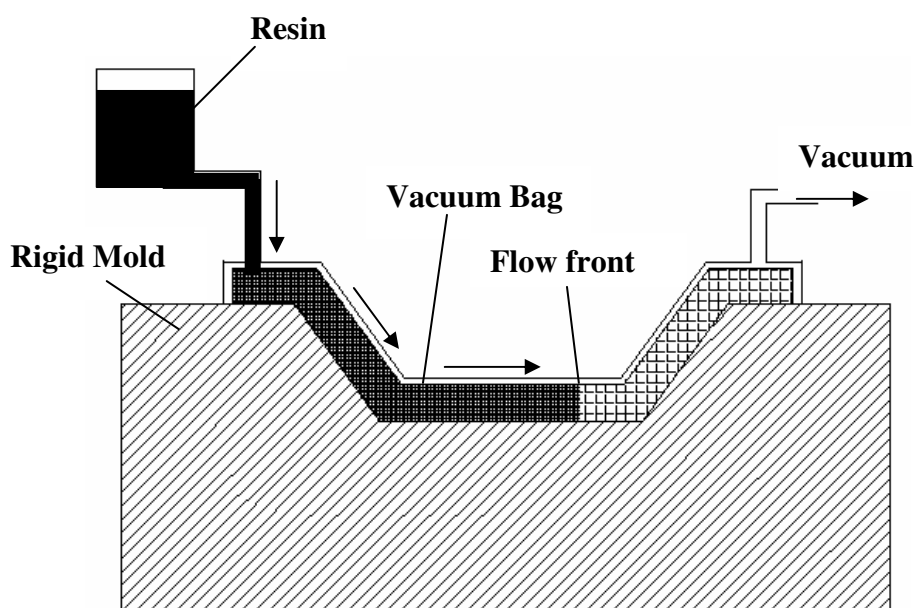


Figure 4.3. Schematic illustration of VARTM process

The difference between in VARTM and RTM process is that in VARTM process, resin is drawn into a preform through use of a vacuum, rather than pumped in under pressure as shown in Figure 3. VARTM does not require high heat or pressure. For that reason, VARTM operates with low cost tooling, making it possible to inexpensively produce large, complex parts in one shot.

The VARTM process has been used in many applications because of its time saving and cost effective characteristics. This process is being currently used in many of the applications in the general aviation industry, defense sector and in the transport industry.

## 4.4. Compression Molding

Compression molding is a high volume process that employs expensive but very durable steel dies. Matched die molding is an alternative name for compression molding. There are three types of compression molding: preform molding, sheet molding compound (SMC) molding and bulk molding compound (BMC) molding. In preform molding, a dry mat of reinforcing material is preformed and placed in the open mold. Resin is added to the preform and the mold halves are then pressed together and heated to cure the part (Figure 4). During the process the resin flows, impregnates the preform, and becomes hard.

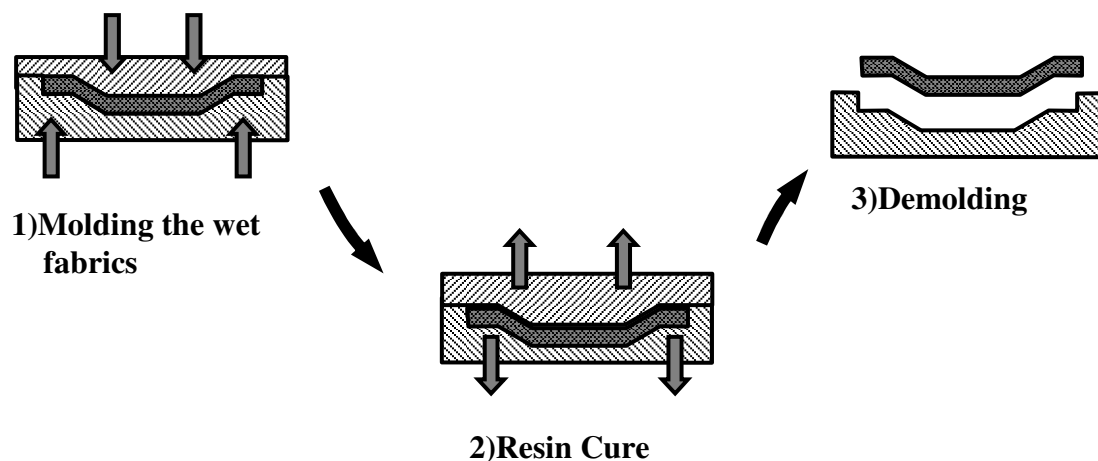


Figure 4.4. Schematic illustration of preform molding

The cured part is removed after the mold is opened. Higher fiber volume fractions may be obtained than in lay up because high pressures can be exerted upon the material, and this results with a stronger part. The cure time in the mold depends on the temperature, the resin type, the part geometry and the mold heating and cooling efficiency. Preforms can be made by cutting the desired shape out of mat or fabric (Lee 1990). With sheet molding compound (SMC) molding, a composite sheet material made by sandwiching chopped fibers between two layers of thick resin paste. To form the sheet, the resin paste transfers from a metering device onto a moving film carrier. Chopped glass fibers drop onto the paste, and a second film carrier places another layer of resin on top of the glass. Rollers compact the sheet to saturate the glass with resin

and squeeze out entrapped air. The resin paste initially is the consistency of molasses over the next three to five days, its viscosity increases and the sheet becomes leather like which is ideal for molding (Dawson 2006). Bulk molding compound (BMC) is a doughlike mixture of chopped fibers, resin, initiator and filler that has a composition similar to that of SMC. The fiber content of BMC is generally is lower than that of SMC and structures made from BMC are not as strong as they would be if made from SMC.

With compression molding high production rates can be obtained with low labor costs. Using a closed mold gives better dimensional control and stability than open mold processes. Higher pressures require more expensive tooling than is necessary for hand lay-up but less expensive tooling than is needed for injection molding (ASM International 1987). With this technique production of complex shapes are possible and both exterior and interior surfaces are finished. Besides these, there is a more equipment need than for layup and compression molding is a more expensive method than layup (Lee 1990).

## CHAPTER 5

### EXPERIMENTAL

#### 5.1. Materials

E-glass non-crimp fabrics, epoxy thermosetting resin and Na<sup>+</sup> montmorillonite clay were used to fabricate composite panels. The reinforcement constituent of composites, E-glass 0°-90° biaxial non-crimp fabrics were provided from Telateks Inc., İstanbul. As the matrix part, DGEBA (diglycidyl ether of bisphenol A) type epoxy resin with an amine curing agent was used. Na<sup>+</sup> montmorillonite clay nanoparticles (MMT, K-10, Aldrich) with a cation exchange capacity of 120 meq/100g were purchased to obtain a nanocomposite matrix. Hexadecyltrimethylammonium chloride (HTAC, Aldrich) with 25 wt. % sol. in water and hydrochloric acid were used for the modification of MMT particles.

#### 5.2. Surface Modification of Montmorillonite Clay

400 mL distilled water at 80<sup>0</sup>C was poured into 20 grams of clay (MMT) and stirred using a magnetic stirrer. Also, a solution of HTAC and hydrochloric acid (HCl) in 100 ml deionized water was prepared. When the acid and HTAC solution reached to 80<sup>0</sup>C, they were mixed and stirred for 1 hour at 80<sup>0</sup>C. The mixture was then filtered and washed with deionized water until no chloride was detected. Residual chloride in the mixture was determined by using AgNO<sub>3</sub>. After the washing procedure is completed, the mixture was filtered and dried for three days at 75<sup>0</sup>C.

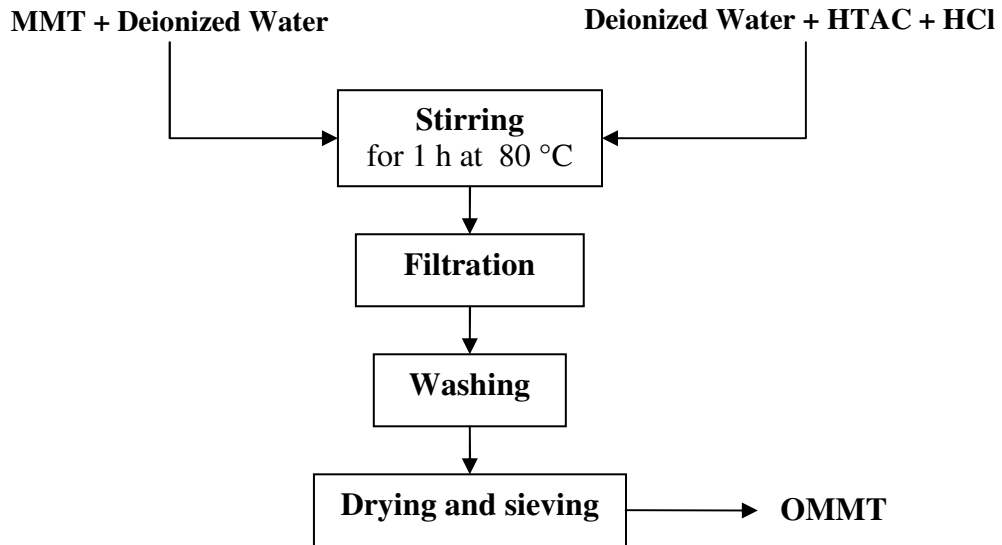


Figure 5.1. Surface treatment route for montmorillonite

### 5.3. Preparation of Layered Silicate/Epoxy Suspension

Layered silicate/epoxy nanocomposite resin systems were prepared with 1, 3, 6, and 10 %wt. of MMT and OMMT to apply them as the matrix for fabric reinforced composites as illustrated in Figure 5.1. In order to enhance the dispersion, the silicate/epoxy suspensions were mechanically stirred for about 1 hour at room temperature. After mechanical stirring, the suspension was hold in an ultrasonic bath for 20 minutes in order to further exfoliate the silicate plaques within the resin. Then, a stoichiometric amount (35 parts curing agent: 100 parts epoxy by weight) of the amine curing agent was added to the suspension. Outgassing procedure was applied by vacuuming to remove bubbles within the resin.

### 5.4. Composite Fabrication

Figure 5.3 illustrates the flowchart of composite fabrication. Hand lay-up technique was used to impregnate and laminate the composite structures. Four plies non-crimp glass fabric were cut in 250 x 250 mm dimensions. Epoxy blend or layered silicate/epoxy suspension was applied as the resin system. The lamination procedure was repeated until all plies were wetted and superimposed. Laminates were cured at

room temperature under a pressure of 8 KPa. A post curing for 1 hour at 80 °C and 2 hours at 150°C was applied in an oven following curing stage.

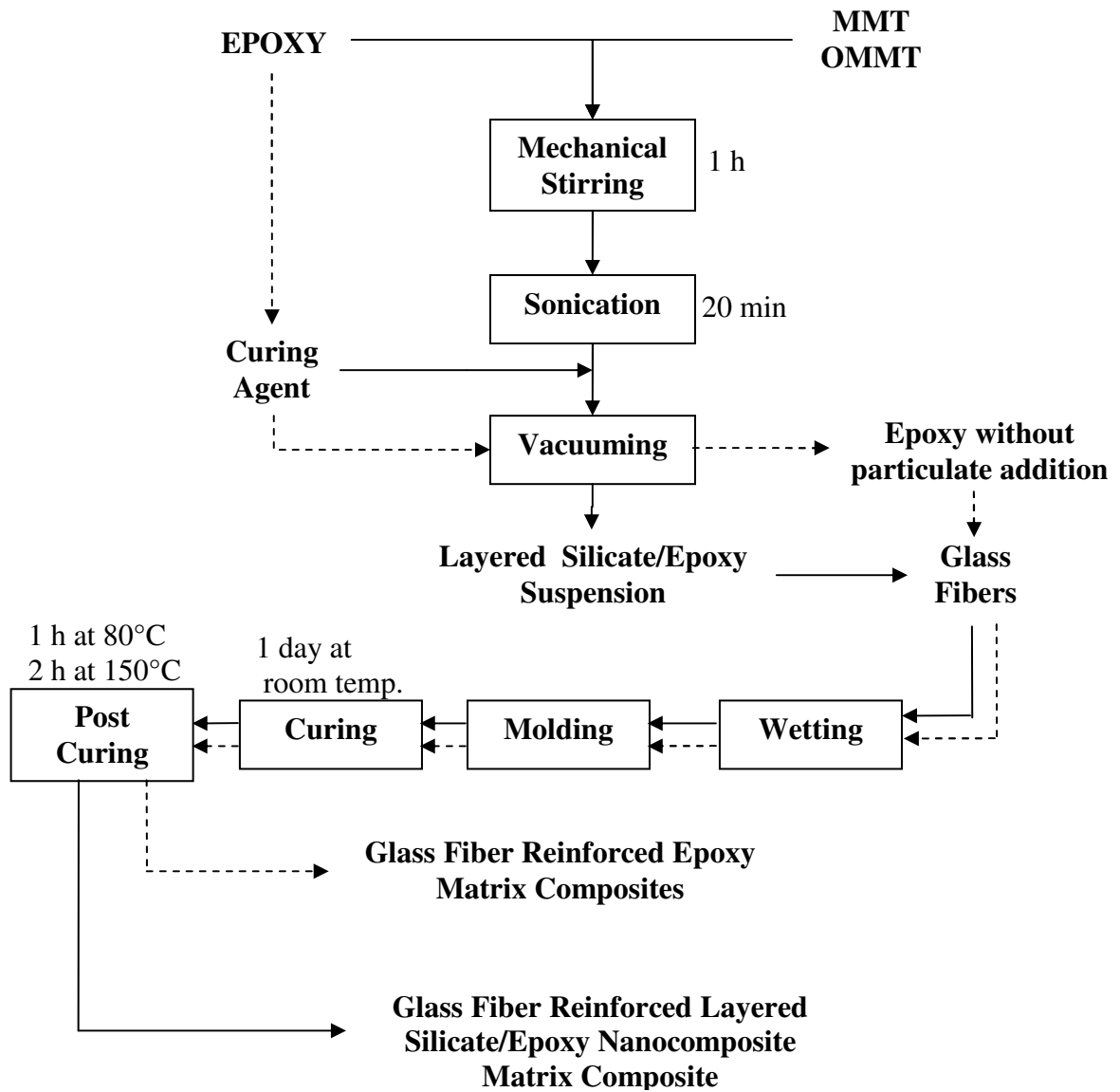


Figure 5.2. Flowchart of composite fabrication process

### 5.5. Fiber Volume Fraction

The fiber volume fractions of the composite panels were measured using the matrix burn out method. Measured weights of composite samples were burned in a

furnace at about 650°C. Then, the remaining fiber mass was weighed and the volume fraction of the fiber was calculated by dividing the mass of the fiber by the density of the fiber material. Fiber volume fraction ( $V_f$ ) of the laminates were calculated based on the following equation;

$$V_f = \frac{v_f}{v_f + v_m} \times 100 = \frac{\frac{m_f}{\rho_f}}{\left( \frac{m_f}{\rho_f} + \frac{m_m}{\rho_m} \right)} \times 100 \quad (5.1)$$

where,  $v_f$  and  $v_m$  are volume of the fiber and matrix,  $m_f$  and  $m_m$  are the mass of fiber and matrix and  $\rho_f$  and  $\rho_m$  are density of fiber and matrix, respectively.

## 5.6. Microstructure Characterization

### 5.6.1. X-Ray Diffraction (XRD)

Montmorillonite particles with and without surface modifications and composite samples prepared with MMT or OMMT using various concentrations (0, 1, 3, 6 and 10 wt. %) were analyzed by X-ray diffraction (XRD) technique using Philips X'Pert Pro diffractometer, with CuK $\alpha$  radiation. Powdered samples were scanned in the interval of  $2\Theta = 2^\circ - 12^\circ$  at 40 kV and 30 mA. Using XRD, interlayer spacing of silicate layers and intercalation behaviour of silicate particles were analyzed.

### 5.6.2. Scanning Electron Microscopy (SEM)

Scanning electron microscopy analyses were performed in order to examine the fracture surfaces of laminates manufactured with and without nanoparticles. By examining the fracture surfaces of laminates, interfacial properties between glass fibers and layered silicate/epoxy matrix, agglomeration behaviour of silicate layers and the

effect of particule loading on the fracture mechanisms were investigated. Samples were gold coated before they were observed in SEM.

### **5.6.3. Optical Microscopy**

Optical microscopy on the polished surface of laminates was performed in order to observe fiber alignment of non-crimp glass fabrics and to investigate the void content in the composite. For this purpose, Nikon™ optical microscope was used. To measure the areal fraction of the voids on the polished surfaces, an image analyzer software was used.

## **5.7. Mechanical Property Characterization**

### **5.7.1. Tensile Test**

Tensile test technique, ASTM D 3039M-93 was used to determine the tensile strength and modulus of the composites. Test specimens were sectioned from the composite panels with the width of 25 mm, thickness of 4 mm and length of 220 mm. At least five specimens were prepared using a diamond saw for each set of composites with MMT or OMMT (1, 3, 6 and 10 wt. %). The specimens were tested using Shimadzu AGI universal test machine at a cross head speed of 2 mm/min (Figure 5.3). The tensile strength ( $\sigma$ ) values were calculated using the following equation;

$$\sigma = \frac{F}{A} \quad (5.2)$$

where F is the applied load, and A is the cross sectional area of the specimen. Elastic modulus was obtained from the initial portion of stress ( $\sigma$ )- strain ( $\epsilon$ ) graphs based on the equation below is given by;

$$E = \frac{\sigma}{\epsilon} \quad (5.3)$$

A video extensometer was used to obtain strain values. Strain values ( $\epsilon$ ) were calculated from;

$$\epsilon = \frac{(L - L_0)}{L_0} \quad (5.4)$$

where  $L_0$  is the distance between gage marks on the samples at the beginning of the testing, and  $L$  is the distance between gage marks obtained with the extensometer at a specific time during the extension.



Figure 5.3. Tensile test specimen under load

### 5.7.2. Flexural Test

The flexural test technique according to ASTM D 790M-86 was used to determine flexural strength and modulus of the composites in order to investigate the effects of clay loading on flexural properties. The flexural test specimens with 10 mm in width, 4 mm in depth and 80 mm in length were sectioned from the composite laminates. At least five specimens from laminates including 1, 3, 6 and 10 wt. % of MMT and OMMT clay particules in the epoxy matrix and laminates manufactured with neat epoxy matrix were tested using the Schimadzu AGI universal test machine with the cross head speed of 1.7 mm/min. Specimens were tested with a 3-point bending apparatus with a span to thickness ratio of 16 (Figure 4). Force vs. deflection at the

center of the beam was recorded. The flexural strength,  $S$ , values were calculated using the equation below;

$$S = \frac{3PL}{2bd^2} \quad (5.5)$$

where  $P$  is the applied load at the deflection point,  $L$  is the span length,  $d$  and  $b$  are the thickness and the width of the specimen, respectively. The maximum strain in the outer fibers occurs at midspan and calculated as;

$$r = \frac{6Dd}{L^2} \quad (5.6)$$

where  $r$  is the maximum strain in the outer fibers,  $D$  is the deflection of the center of the beam. The Flexural modulus values,  $E_b$ , were calculated from;

$$E_b = \frac{L^3 m}{4bd^3} \quad (5.7)$$

where  $m$  is the slope of the tangent to the initial straight line portion of the load-deflection curve.

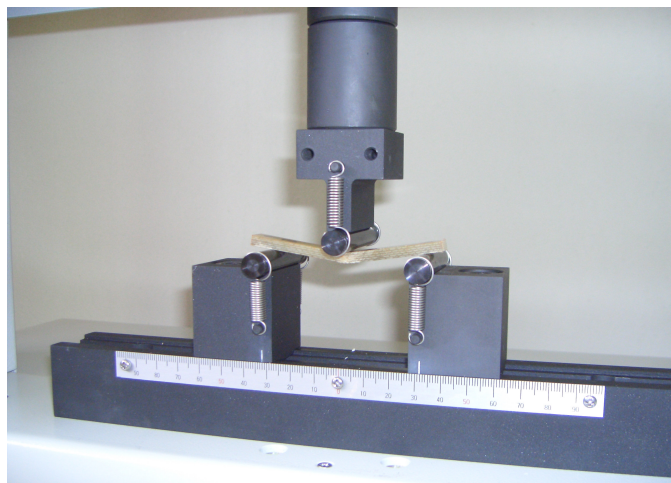


Figure 5.4. Flexural testing specimen under loading

### 5.7.3. Short Beam Shear (SBS) Test

The apparent interlaminar shear strength of composite laminates was determined using a Short Beam Shear (SBS) test in accordance with ASTM D2344-84. Eight specimens from each set were tested using the Shimadzu AGI universal test machine with the cross head speed of 1.3 mm/min. The short beam shear specimens; 4 mm in thickness, 6.5 mm in width and 30 mm in length were sectioned from the composite laminates. The length to thickness ratio and span to thickness ratio were kept constant at 7 and 5, respectively. SBS test configuration is shown in Figure 5. The apparent shear strength ( $\tau_{\max}$ ) was calculated using the following equation.

$$\tau_{\max} = \frac{0.75P_B}{bd} \quad (5.8)$$

where  $P_B$  is the breaking load,  $b$  and  $d$  are width and the thickness of the specimens., respectively.

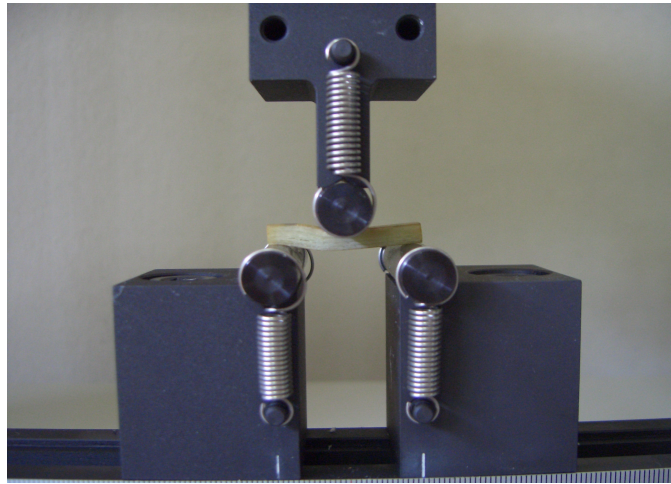


Figure 5.5. SBS test configuration

### 5.7.4. Fracture Toughness ( $K_{IC}$ ) Test

To investigate the effect of clay loading on mode I interlaminar fracture toughness ( $K_{IC}$ ) of composite laminates, Single Edge Notched Bending (SENB) method, D5045-91a was used for this purpose. The SENB specimens were obtained from composite laminates with 8 mm in width, 4 mm in thickness and 40 mm in length. The crack length,  $a$ , was selected such that  $0.45 < a/W < 0.55$ , where  $W$  is the thickness of composite laminate as sketched in figure 6.

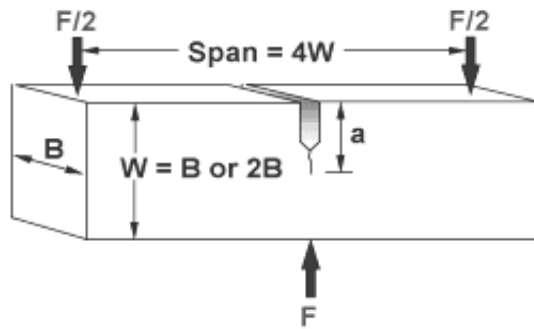


Figure 5.6. Fracture toughness test specimen (Source:WEB\_3 2006)

The specimens were tested using a 3-point bending apparatus with the cross-head speed of 10 mm/min and span length,  $S$ , was fixed as four times the width. Mode I fracture toughness ( $K_{IC}$ ) values were calculated with the following equation.

$$K_{IC} = (P_Q BW^{1/2})f(x) \quad (5.9)$$

where  $P_Q$  is the applied load,  $B$  is the specimen thickness,  $W$  is the specimen width,  $f(x)$  is the calibration factor that can be determined as follows:

$$f(x) = 6x^{1/2} \frac{[1.99 - x(1-x)(2.15 - 3.93x + 2.7x^2)]}{(1+2x)(1-x)^{3/2}} \quad (5.10)$$

where  $x = a/W$  and  $0 < x < 1$ .

## **5.8. Thermal Property Characterization**

### **5.8.1. Differential Scanning Calorimetry (DSC)**

The differential scanning calorimeter (DSC) is an analytical tool that measures the heat flux to a material sample as it is maintained at a constant temperature or along a linear temperature ramp. The DSC operates by comparing the heat transfer to the sample pan with the heat transfer to a reference pan. From this heating data, physical properties such as melting point, glass transition point, and reaction kinetics can be determined. DSC analysis was conducted to samples obtained from each laminate, on a TA instrument Q10 model DSC under nitrogen atmosphere at a flow of 50mL/min in order to investigate the effect of clay loading on the glass transition temperature ( $T_g$ ). To conduct DSC analysis, 5-6 mg of each specimen was put in an aluminum pan and placed in the instrument. The dynamic measurements were made at a constant heat rate of 10°C/min from 25 to 200°C.  $T_g$  of laminates manufactured with epoxy matrix including different amounts of MMT and OMMT were calculated by the midpoint method.

### **5.8.2. Dynamic Mechanical Analysis (DMA)**

Dynamic mechanical analysis (DMA) measures the mechanical properties of materials, particularly polymers. DMA determines elastic modulus (or storage modulus,  $E'$ ), viscous modulus (or loss modulus,  $E''$ ) and damping coefficient ( $\tan \delta$ ) as a function of temperature, frequency or time. DMA identifies transition regions in plastics, such as the glass transition, and may be used for quality control or product development. DMA can recognize small transition regions that are beyond the resolution of DSC (Differential Scanning Calorimetry). The test specimen is clamped between the movable and stationary fixtures, and then enclosed in the thermal chamber. Frequency, amplitude, and a temperature range appropriate for the material being tested are input. The Analyzer applies the oscillation force to the test sample while slowly moving through the specified temperature range.

The DMA specimens; 2.5 mm in thickness, 12 mm in width and 55 mm in length were sectioned from the composite laminates and tests were conducted with multifrequency-strain mode with a strain rate of 0.1%. While testing dual cantilever clamp were used and a heating rate of 2°C/min from 25 to 150°C was applied.

### 5.8.3. Flame Retardancy

The UL 94 test determines the material tendency to extinguish or to spread the flame once the specimen has been ignited. This test method covers a small scale laboratory screening procedure for comparing the relative rate of burning and/or extent and time of burning of self supporting plastics in the form of bars. A specimen is supported in a horizontal position and is tilted at 45° as shown in Figure 7. The specimens were sectioned from composite laminates 10 mm in width, 4 mm in thickness and 125 mm in length according to ASTM D635-91. A flame is applied to one end of the specimen to produce a blue flame of 20 mm high for 30 seconds or until the flame reaches the 25 mm mark. If the specimen continues to burn after the removal of the flame, the time for the specimen to burn between the 25 mm and 100 mm marks are recorded. If the specimen stops burning before the flame spreads to the 100 mm mark, the time of combustion and damaged length between the two marks is recorded.

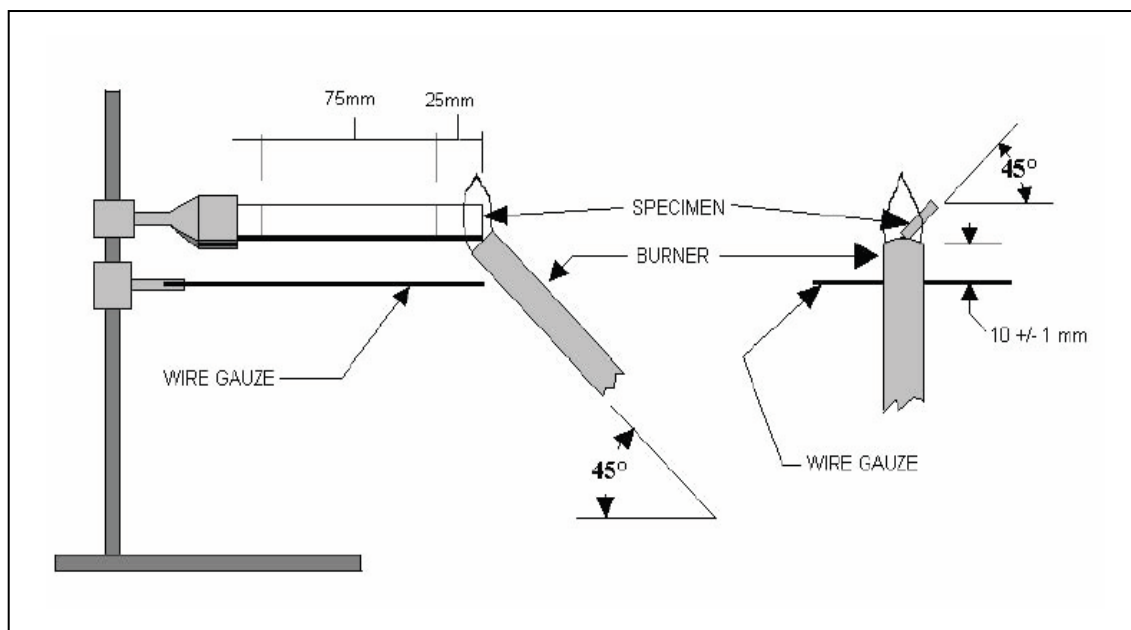


Figure 5.7. UL94 Horizontal burn set up (Source: WEB\_4 2006)

The burning rate of the specimen can be calculated as;

$$\text{Burning Rate} = \frac{L}{(t - t_1)} \quad (5.11)$$

where L is the burned length after the 25 mm mark, t is the burning time, and t<sub>1</sub> is the burning time when the flame front reaches the 25 mm mark. The extent of burning is defined as 100 mm minus the unburned length. Average extent of burning and average time of burning can be calculated with the following equations.

$$AEB, mm = \frac{\Sigma(100 mm - \text{unburned length})}{(\text{number of specimens})} \quad (5.12)$$

$$ATB, mm = \frac{\Sigma(t - t_1)}{(\text{number of specimens})} \quad (5.13)$$

where, t and t<sub>1</sub> refers to the burning time and the time taken when the flame front reaches the 25 mm mark, respectively.

## CHAPTER 6

### RESULTS AND DISCUSSION

The effects of modification of the matrix material with silicate nanolayers on the mechanical, thermal and flame retardant properties of non crimp E-glass/epoxy were investigated and the results are given in this chapter. As mentioned in Chapter 5, non-crimp fiber (NCF) reinforced epoxy composites were manufactured with hand lay-up technique and cured under a pressure of 8 KPa in a mold. This manufacturing process eliminates the problems associated with the increase in the viscosity of nanoparticle added matrix as well as filtering of particules by fabrics and incomplete wetting of fibres. Composites were laminated with five plies of 0°/90° biaxial NCFs and epoxy in various type illustrated in Table 6.1.

#### 6.1. Fiber Volume Fraction and Void Content

Fiber volume fraction of the composites were determined by matrix burn out method and void contents of laminates were determined by performing an image analysis on the optical microscopy images of each laminate cross-sections. As tabulated in Table 1, fiber volume fractions ( $v_f$ ) varied between 40 and 44 % in the composites.

Table 6.1. Fiber volume fraction and void contents of composite laminates fabricated with various concentrations of silicates.

NCF/epoxy Composite	MMT					OMMT				
	0	1	3	6	10	0	1	3	6	10
Silicate concentration (wt.%)	0	1	3	6	10	0	1	3	6	10
Fiber volume fraction, $V_f$ (%)	44.3	41.5	41.5	42.3	40.6	44.3	42.1	40.6	43.6	42.3
Void content (%)	3.7	3.9	5.6	6.3	6.4	3.7	4.1	6.5	5.6	6.6

An example of optical micrographs of the laminates and their binary image forms are shown in Figures 6.1 and 6.2, respectively. The contrast difference in the binary images was related to the void regions. It was found that the void content of the

composites increased with increasing silicate content. This was due to the increase of the viscosity of the matrix and entrance of air bubbles through the silicate particles. As it is also seen from Table 6.1, the increase of void content of the composites prepared with OMMT/epoxy matrix is higher than that of prepared with MMT/epoxy matrix. The void formation was greater in OMMT/epoxy matrix due the presence of surfactant used in the surface treatment of silicate particles.

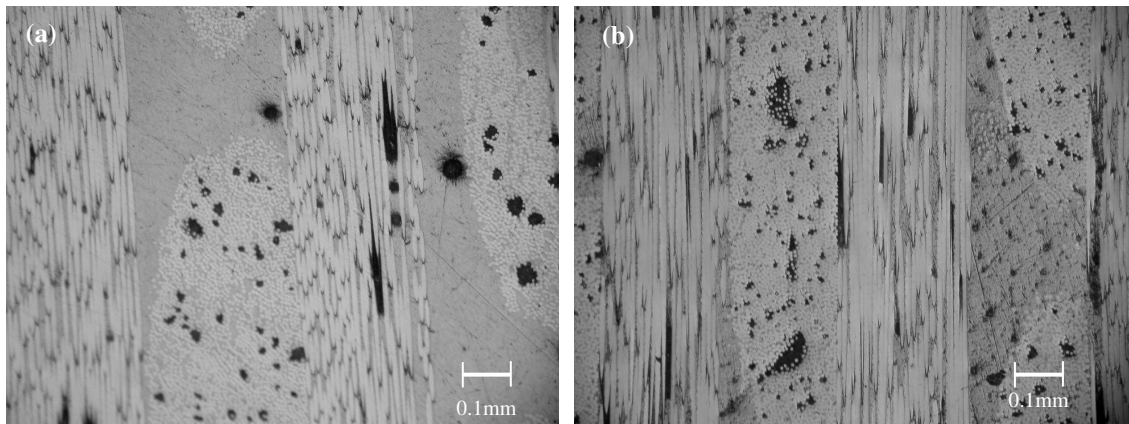


Figure 6.1. Optical micrographs of (a) NCF/neat epoxy composites (b) NCF/3 wt.% OMMT/epoxy composites

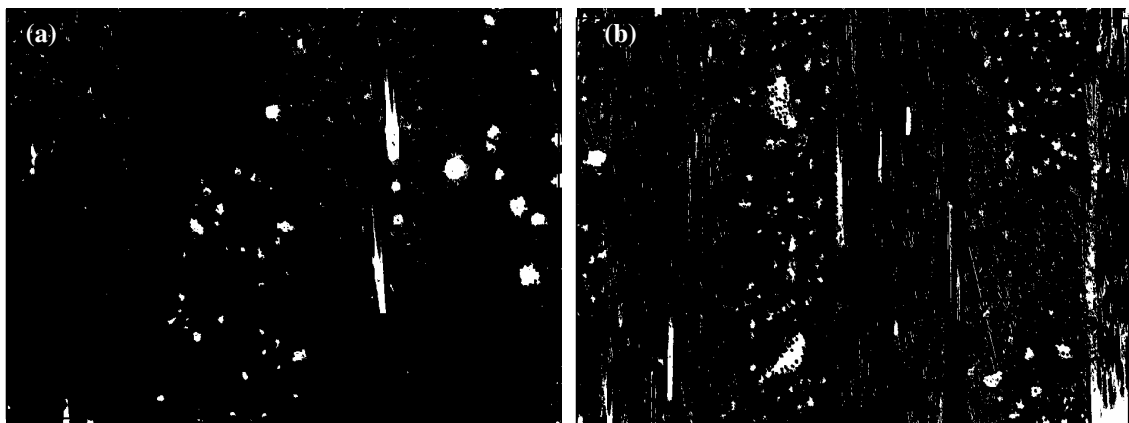


Figure 6.2. Transformed binary images of (a) NCF/ neat epoxy composite (b) NCF/3 wt.% OMMT/epoxy composites

## 6.2. Microstructural Development

X-ray diffractograms of surface treated (OMMT) and untreated (MMT) silicate particles are shown in Figure 6.3. The MMT and OMMT have characteristic peaks at  $2\theta = 6.17^\circ$  and  $2\theta = 4.87^\circ$ , respectively and the peaks correspond to the (001) plane reflections of clays. The OMMT particles have a d-spacing of  $18.1 \text{ \AA}$ , while the d-spacing of untreated silicates are  $14.3 \text{ \AA}$ . Exchange of sodium cations by the onium cations results with the increase of the interlayer spacing of silicate particles and create organophilic surfaces and hence better compatibility with the epoxy resin and curing agent.

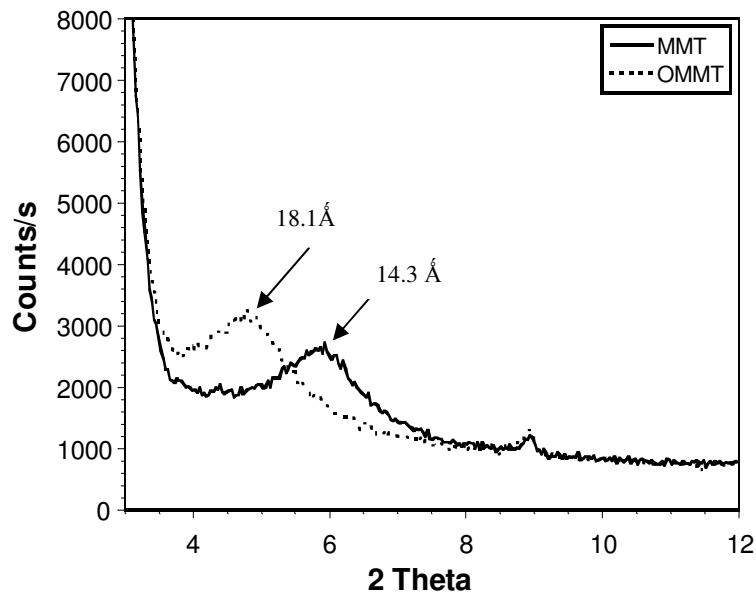


Figure 6.3. X-ray diffractograms of MMT and OMMT silicates

Figures 6.4 and 6.5 illustrate the XRD diffractograms of the glass fiber reinforced laminates manufactured with neat epoxy, MMT/epoxy and OMMT/epoxy nanocomposites. The characteristic peaks of silicates illustrated in Figure 6.3 are not visible for the composites. This is due to further intercalation of the silicates during the polymerization of the resin and a relatively good dispersion of silicate particles in the epoxy matrix.

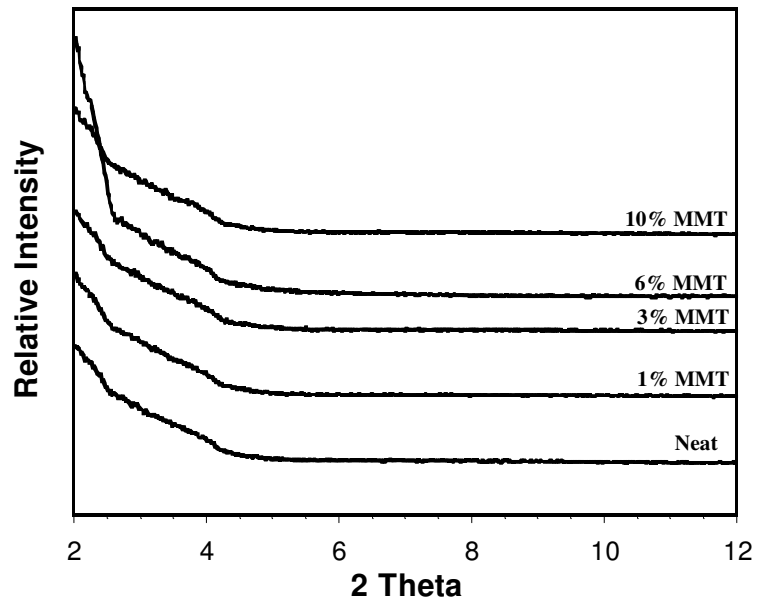


Figure 6.4. X-ray diffractograms of glass fiber reinforced MMT/epoxy nanocomposites

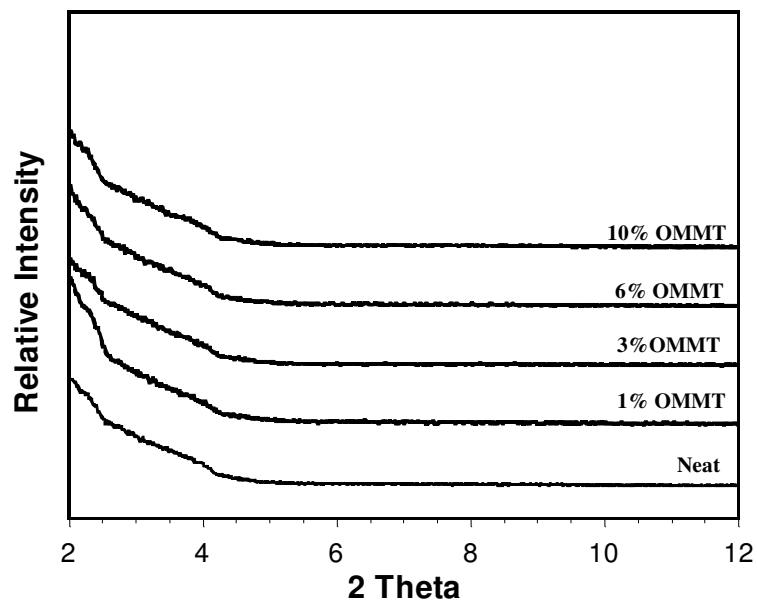


Figure 6.5. X-ray diffractograms of glass fiber reinforced OMMT/epoxy

## 6.3. Effects of Silicate Layers on the Mechanical Properties of the Composites

### 6.3.1. Tensile Properties

Figures 6.6 and 6.7 show the tensile stress vs. strain response of E-glass/epoxy composites containing different concentrations of modified and unmodified silicate particles, respectively. Stress- strain response of all laminates is non-linear and there is a sudden drop after the maximum stress at which failure occurs. Figures 6.8 and 6.9 exhibit the tensile strength and elastic modulus of the composites. It was found that the laminates with MMT exhibit slightly higher strength values as compared to those with OMMT. The tensile strength and modulus values remain almost constant by the addition of MMT and OMMT up to 6 wt. % silicate contents as compared to those fabricated without silicate addition. However, further addition of MMT and OMMT reduces the strength values. On the other hand, modulus values are reduced by the addition of OMMT while they remains constant with MMT addition at 10 wt. % silicate loading.

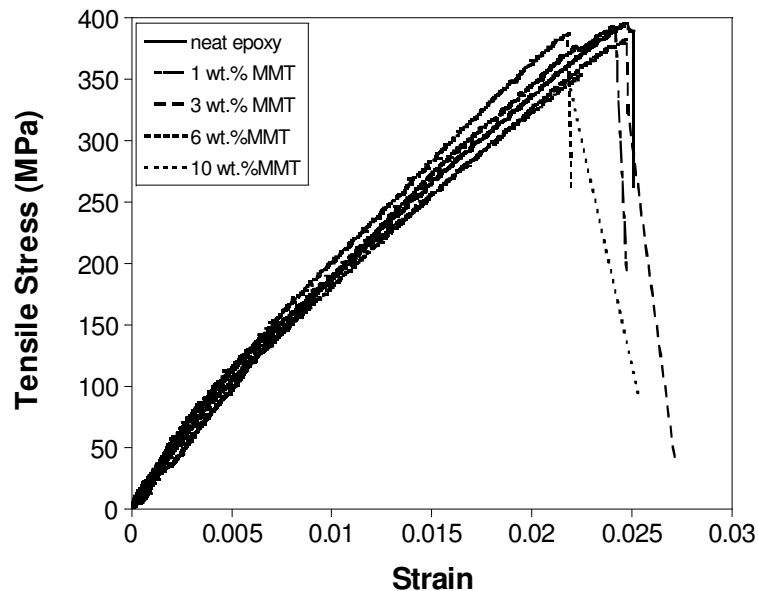


Figure 6.6. Tensile stress vs. strain response of composites with and without MMT loading

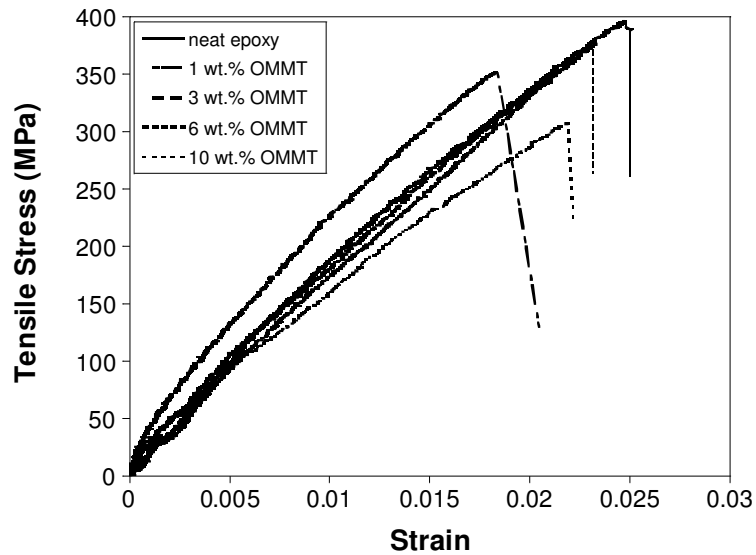


Figure 6.7. Tensile stress vs. strain response of composites with and without OMMT loading

This results indicates that modifying the matrix of non-crimp fabric reinforced epoxy composites with layered silicates has no significant effect on the tensile properties due to the dominating effect of fiber reinforcement. These reductions in both tensile strength and modulus might caused by the higher void content in composites at high silicate concentration. Similar behaviour was observed with the addition of carbon nanotubes to the matrix of glass fiber reinforced epoxy composites (Gojny et al. 2005). They showed that tensile strength and modulus of laminates were not affected by the addition of carbon nanotubes.

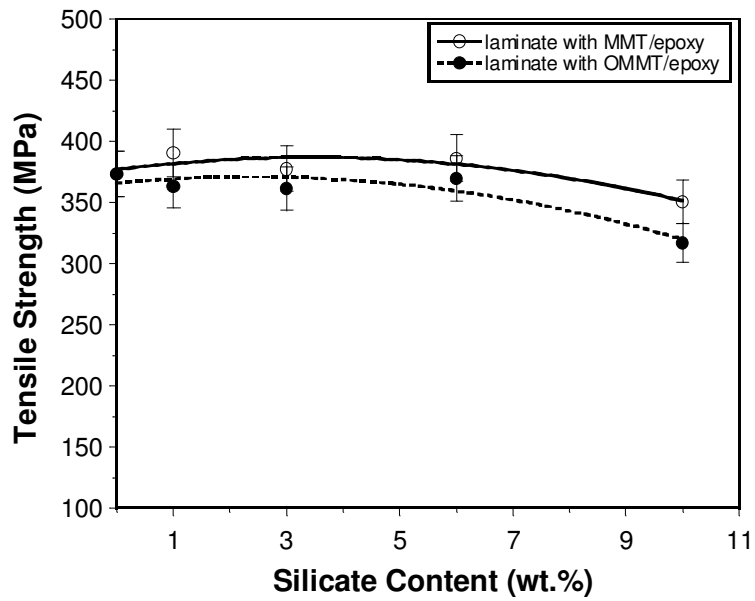


Figure 6.8. Tensile strength of non-crimp glass fabric reinforced epoxy composites with silicate nanoparticle addition

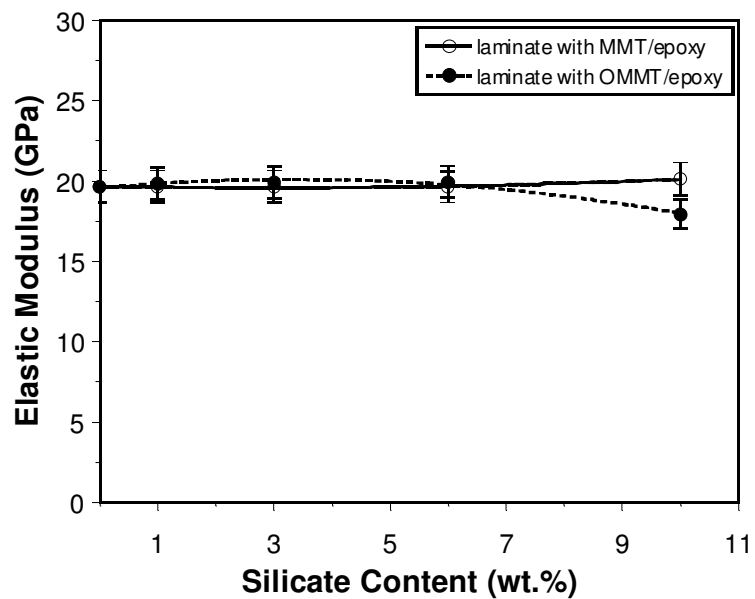


Figure 6.9. Elastic modulus of non-crimp glass fabric reinforced epoxy composites with silicate nanoparticle addition

### 6.3.2. Flexural Properties

Figures 6.10 and 6.11 show the flexural stress and strain responses of composites with OMMT and MMT additions, respectively. Stress values increases linearly and fracture occurs at the peak stress values. Above the maximum stress, the failure is a progressive fracture of fabric layers and local delamination.

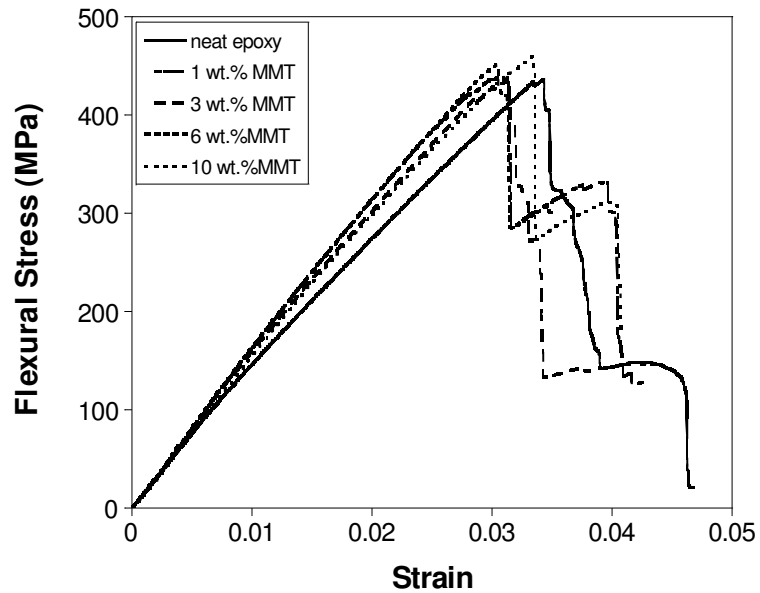


Figure 6.10. Flexural stress vs. strain response of composites with MMT loading

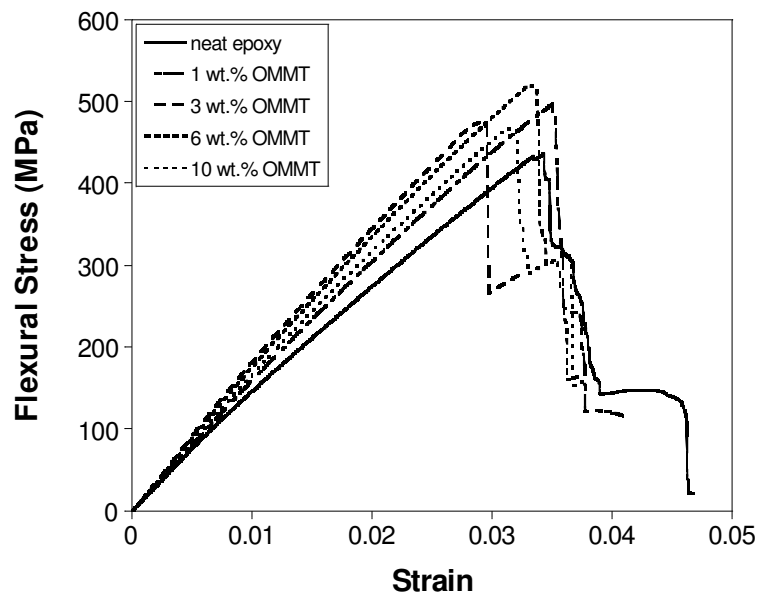


Figure 6.11. Flexural stress vs. strain response of composites with OMMT loading

Figures 6.12 and 6.13 exhibit the influence of silicate loading on the flexural strength and modulus values as a function of silicate loading. Flexural strength and modulus values of composites prepared without silicate addition were measured as, 443 MPa and 16 GPa, respectively. Flexural strength and modulus values increases with the addition of MMT and OMMT, up to 6 wt. % of silicate loading. By the addition 6 wt.% of silicate to the matrix increases the flexural strength to 513 MPa and flexural modulus to 18 GPa. The highest improvement in flexural strength and modulus were found to be by 16 and 13%, respectively by the addition of 6 wt. % of silicates. The improvement in the flexural strength may be related with the presence of silicate layers located at the interface of the fiber and the matrix. The silicate layers may enhances the interfacial properties up to a critical concentration. In bending test, the loading is a mixture of tension, compression and shear. Tensile load opens the voids while compression loads tend to close it. This might be another reason of improved flexural strength up to some concentrations. Kornmann et al. (2005) observed improvement in the flexural strength and modulus by 27 and 6%, respectively, by using a nanocomposite matrix. They obtained this improvement by loading organosilicates to the matrix of glass fiber reinforced composites and this improvement was explained with the presence of layered silicates at the surface of glass fibers, which may improve the interfacial properties between the matrix and the fibers (Kornmann et al. 2005).

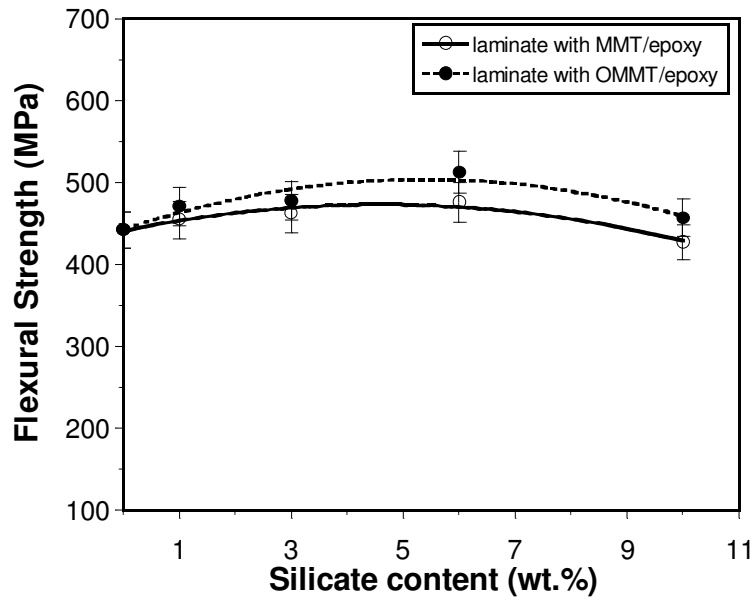


Figure 6.12. Flexural strength of non-crimp glass fabric reinforced epoxy composites with silicate nanoparticle addition

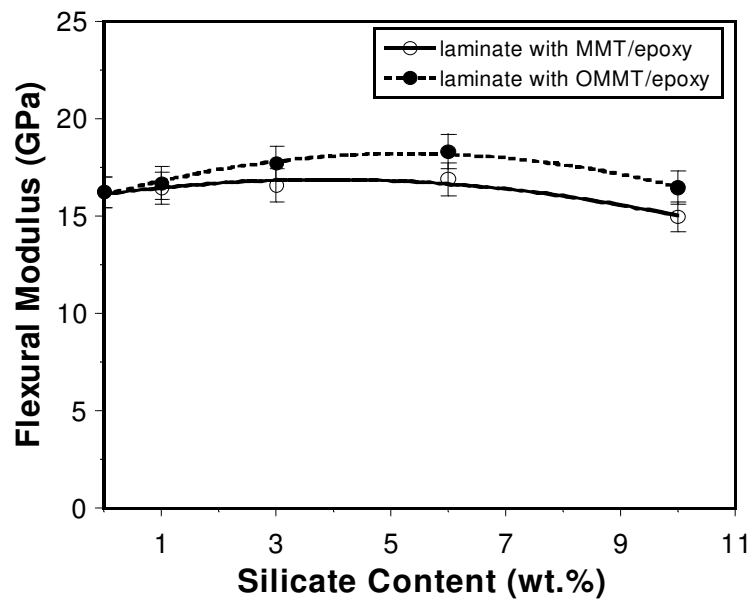


Figure 6.13. Flexural modulus of non-crimp glass fabric reinforced epoxy composites with silicate nanoparticle addition.

Figures 6.14 and 6.15 illustrate the SEM fracture surface images of glass fabric reinforced laminates prepared with neat epoxy and OMMT/epoxy suspension, respectively. As seen in Figure 6.14 (a) and (b), fracture occurs along the interface and smooth fracture surfaces formed due to interfacial debonding and matrix cracking which indicates a lower strength. In contrast, in the case of composites laminated with silicate containing epoxy matrix, it is evident that fracture mechanisms are altered due to the presence of silicates. The fracture modes indicate that a stronger interface is formed in these composites.

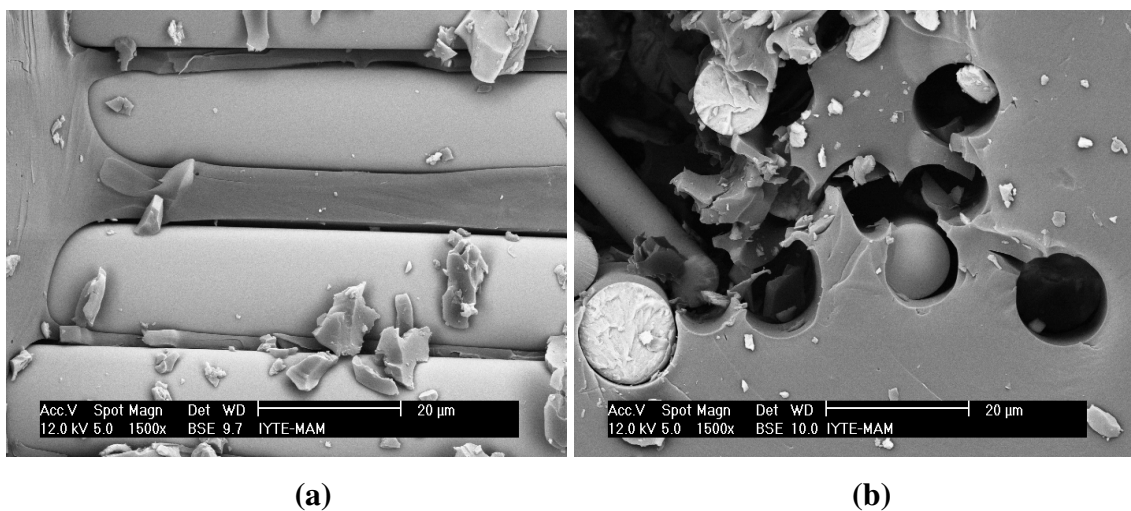


Figure 6.14. SEM fracture surface images of non-crimp glass fiber/epoxy composites

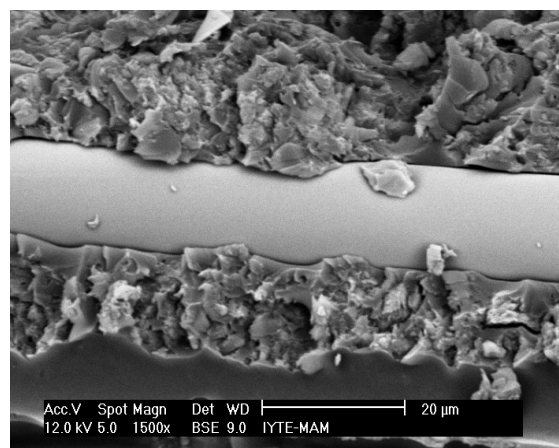


Figure 6.15. SEM fracture surface image of non-crimp glass fiber/epoxy composites with 10 wt. % silicate addition

### 6.3.3. Interlaminar Shear Strength (ILSS)

Short beam shear test was applied to the laminates to determine the interlaminar shear properties of composites prepared with different silicate loading. Figure 6.16 shows the effect of silicate loading on the interlaminar shear strength (ILSS) of composites. Apparent interlaminar shear strength of fabric reinforced composites with neat epoxy matrix was measured as 32.7 MPa. With the addition of silicate particles, ILSS of laminates decreases slightly and the reduction is greater in the case of OMMT particule addition. The reduction may be related with the formation of voids in the matrix which is located at the interlaminar region of composites. The tendency of void formation is higher in OMMT added composites as compared to MMT added ones, as given in Table 6.1. Timmerman et al. (2002) studied the effects of nanoclay reinforcement to the ILSS of carbon fiber/epoxy composites and observed a small increase in ILSS at low clay loadings. At higher loadings of clay ILSS of composites decreased and this was explained such that the more ordered clay particules in the sample act as crack initiators instead of reinforcement (Timmerman et al. 2002).

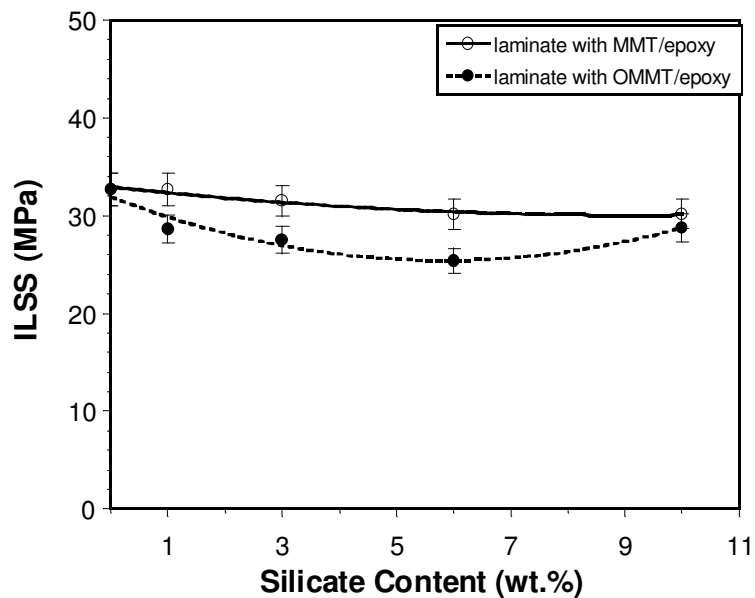


Figure 6.16. ILSS of non-crimp glass fabric reinforced epoxy composites with silicate nanoparticle addition

### 6.3.4. Fracture Toughness ( $K_{IC}$ )

Fracture toughness of laminates containing various concentrations of MMT and OMMT particules were obtained by loading the SENB specimens along in-plane directions. Figure 6.17 shows the fracture toughness ( $K_{IC}$ ) values of composites as a function of clay loading. Fracture toughness of composites laminated with neat epoxy was measured as  $2.8 \text{ MPa}\cdot\text{m}^{1/2}$ . With the addition of OMMT (10 wt.%) particules to the matrix, fracture toughness of laminates increases by 5 %. However, the presence of MMT particules slightly reduces  $K_{IC}$  values. As a result of loadings along the in-plane directions, fiber-matrix debonding, fiber pull-out, fiber and matrix fracture mechanisms were observed to occur in the laminates. A better dispersion and intercalation of OMMT particules may be related with the higher  $K_{IC}$  values measured from composites prepared with OMMT/epoxy matrix. The reduction in  $K_{IC}$  values with the addition of MMT particules may be related to the higher fraction of agglomerates.

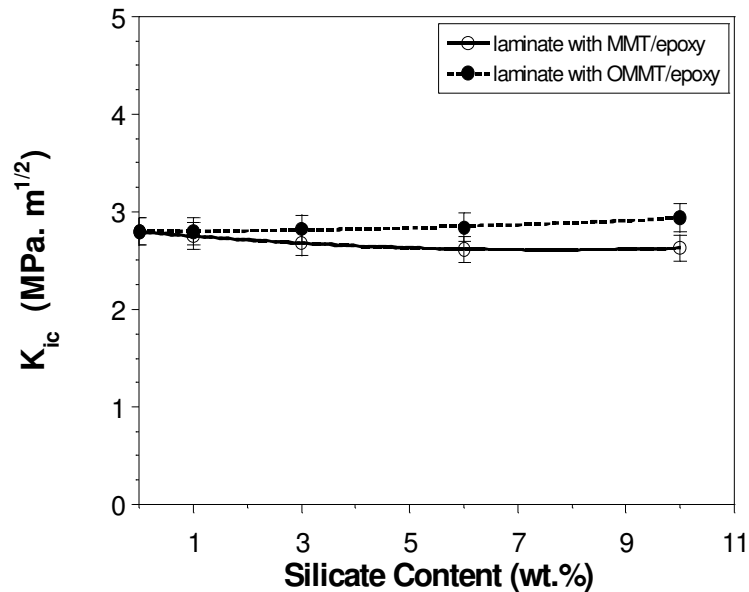


Figure 6.17. Fracture toughness ( $K_{IC}$ ) of non-crimp glass fabric reinforced silicate/epoxy nanocomposites

## 6.4. Thermal Properties

### 6.4.1. Effect of Silicate Loading on the Glass Transition Temperature of Laminates

Glass transition temperatures ( $T_g$ ) of the fabric reinforced composites were measured from DSC analysis and the effect of silicate content on the  $T_g$  values of laminates are shown in Figures 6.18 and 6.19. The  $T_g$  of the laminates without particulate addition was determined as 70°C. Addition of MMT particles to the matrix has almost no effect on the  $T_g$  values as shown in Figure 6.18. Figure 6.19 reveals an increase of  $T_g$  of the composites with OMMT/epoxy matrix.  $T_g$  of the laminates increases by 7 % up to 6 wt.% OMMT silicate loading. Introduction of OMMT silicate nanoparticles restricts the mobility of polymer molecules, and therefore  $T_g$  increases. However, a reduction of  $T_g$  was observed with the addition of higher contents (10% wt. OMMT). Surfactant used for the surface treatment of silicates may have a plasticizing effect on polymer matrix and the excess surfactant at high concentrations may dominate to decrease of the  $T_g$  values. Lin et al. (2006) investigated the thermal characteristics of the epoxy/clay binary composites using DSC. They observed that clay loading increased the  $T_g$  of epoxy resin. According to Lin et al. (2006) the effect on the  $T_g$  indicated a strong interaction at the molecular level between the polymeric molecules and clay layers, which could come only from the macro-intercalated of the clay. Kaya et al. (2006) found that,  $T_g$  of OMMT/epoxy nanocomposites increases at relatively low additions of organically modified silicate (3 wt. %) and they reported that further additions decreases the  $T_g$ .

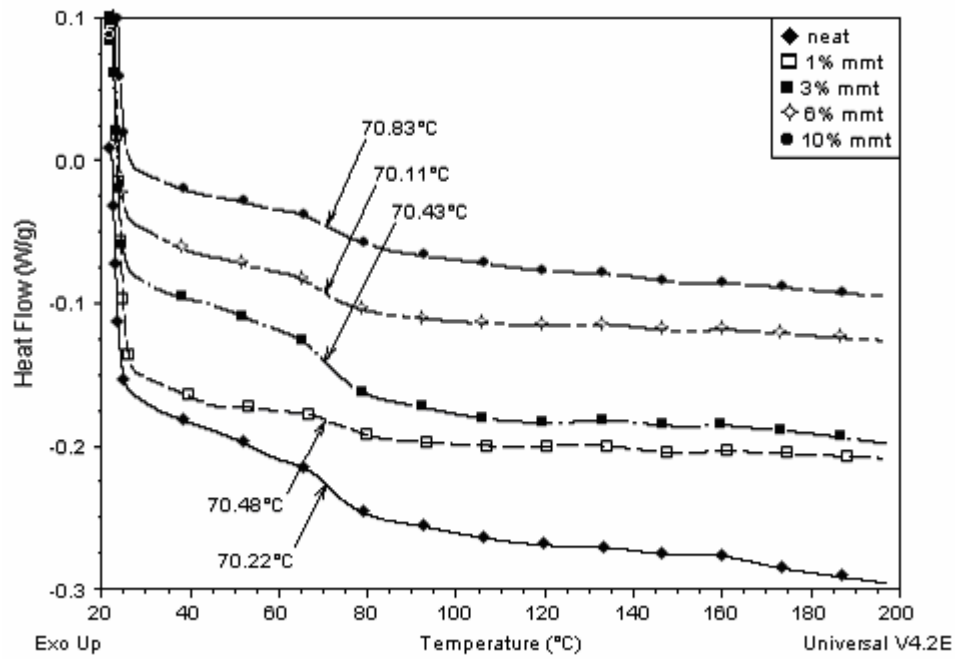


Figure 6.18. DSC thermographs of non-crimp glass fabric reinforced MMT/epoxy nanocomposites

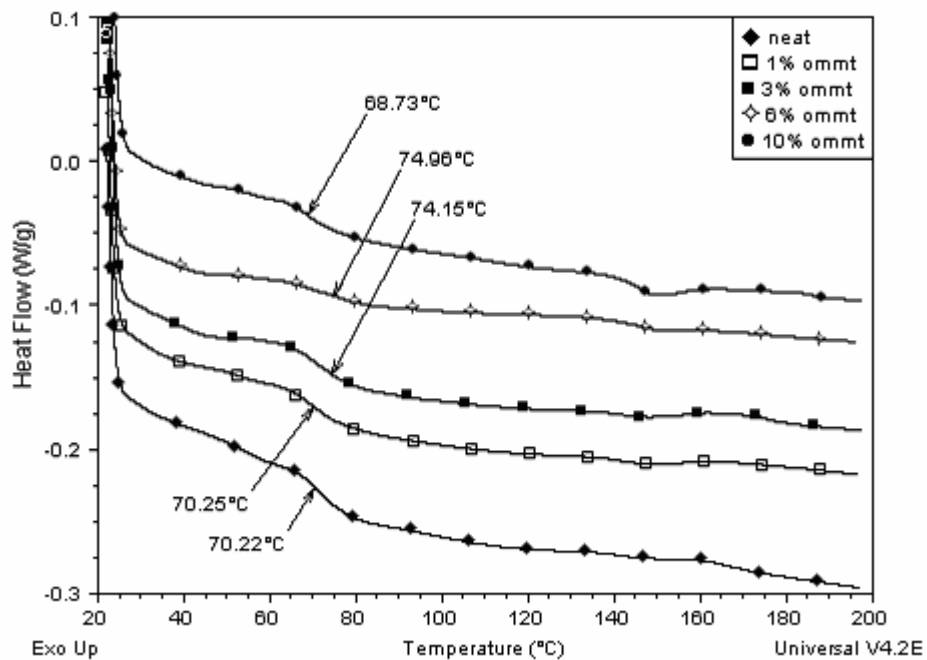


Figure 6.19. DSC thermographs of non-crimp glass fabric reinforced OMMT/epoxy nanocomposites

## 6.4.2. Effect of Silicate Loading on the Thermomechanical Properties of Laminates

The dynamic storage modulus ( $E'$ ), loss modulus ( $E''$ ) and  $\tan \delta$  versus temperature for glass fabric reinforced laminates prepared with neat epoxy and nanocomposites containing 1 wt. % of MMT and OMMT are shown in Figures 6.20 to 6.22, respectively. At around  $T_g$ , the storage modulus values drops significantly and reaches to a constant lower value at further temperatures.

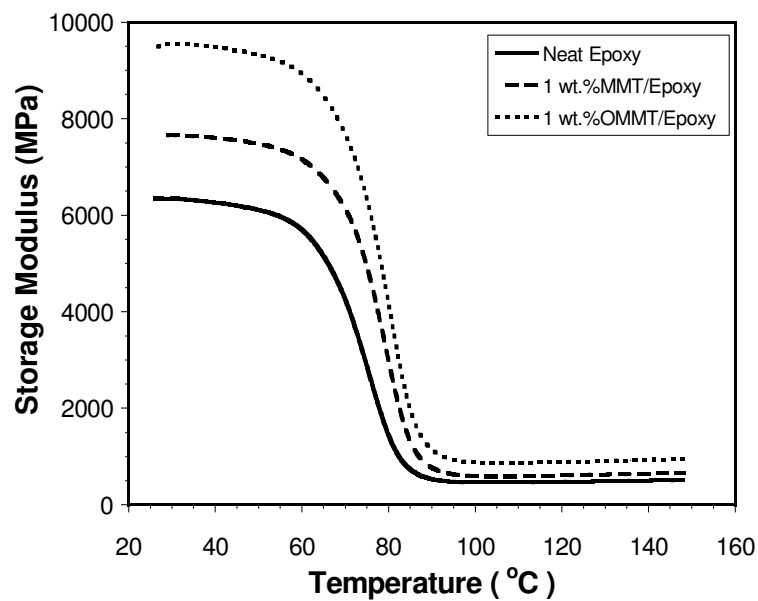


Figure 6.20. Storage Modulus versus temperature plots of non-crimp glass fabric reinforced composites prepared with neat epoxy and nanocomposites containing 1 wt.% MMT and OMMT.

Figures 6.23 exhibit the influence of silicate loading on the storage modulus values as a function of silicate loading. With the addition of silicate particles, the storage modulus of laminates increase up to 6 wt. % silicate content. As a result of incorporation of 6 wt. % of MMT and OMMT silicate particles into the matrix, an increase of about 57 and 51 % in storage modulus were found, respectively. The loss modulus of composites prepared without silicate addition was measured 1.02 GPa as shown in Figure 6.24 and the addition of 6 wt. % of MMT and OMMT to the matrix increased the loss modulus of composites to 1.9 and 1.8 GPa, respectively. In general,

addition of silicate particles increases the storage and loss modulus of composites due to the increased modulus of the matrix.

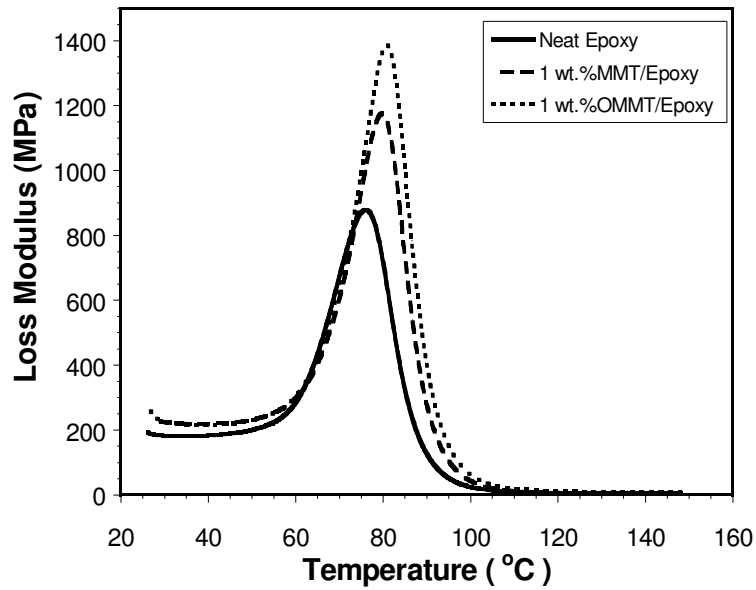


Figure 6.21. Loss Modulus versus temperature plots of non-crimp glass fabric reinforced composites prepared with neat epoxy and nanocomposite containing 1 wt.% MMT and OMMT.

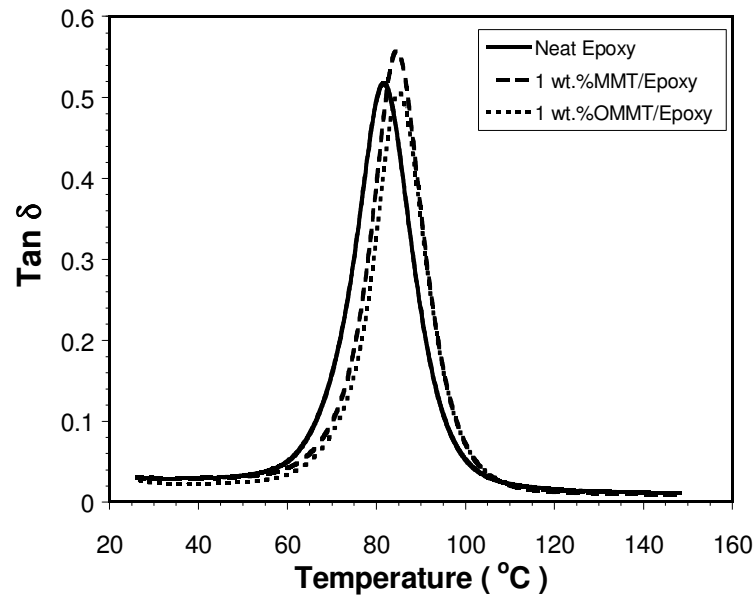


Figure 6.22. Tan  $\delta$  versus temperature plots of non-crimp glass fabric reinforced composites prepared with neat epoxy and nanocomposite containing 1 wt. % MMT and OMMT.

Effects of silicate loading on the thermomechanical properties of glass fiber reinforced composites were studied by Lin et al. (Lin et al. 2006). They reported that the storage modulus in the rubbery plateau region increased with the silicate loading, while the storage modulus in the glassy plateau region was relatively less affected. They related the increased modulus in the rubbery region to the good interfacial bonding between the epoxy and silicates. Chowdhury et al. (Chowdhurt et al. 2006) applied DMA on the nanosilicate/woven carbon/epoxy laminates on a single cantilever beam mode. Similarly, they reported that storage and loss modulus increased with the addition of nanosilicate at low concentrations. An increase of 52 and 47 % was reported for storage and loss modulus at 2 wt. % silicate content, respectively.

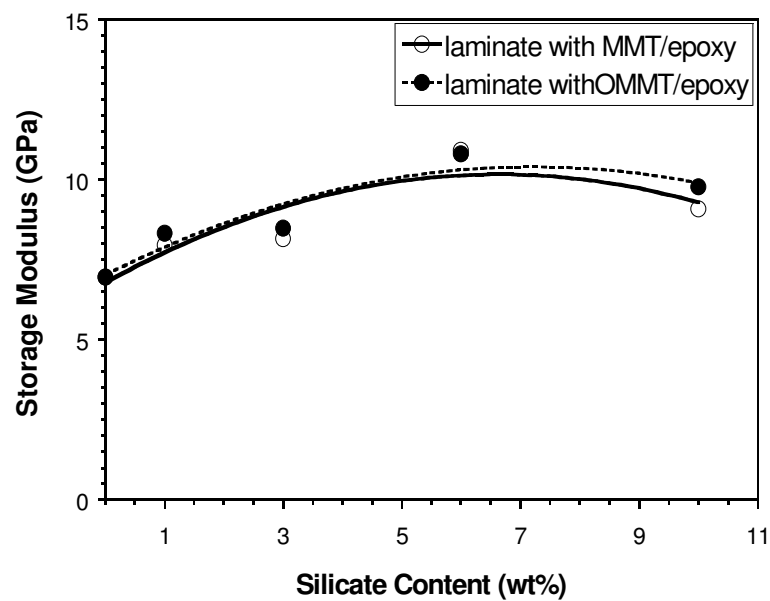


Figure 6.23. Storage modulus of non-crimp fabric reinforced silicate/epoxy nanocomposites

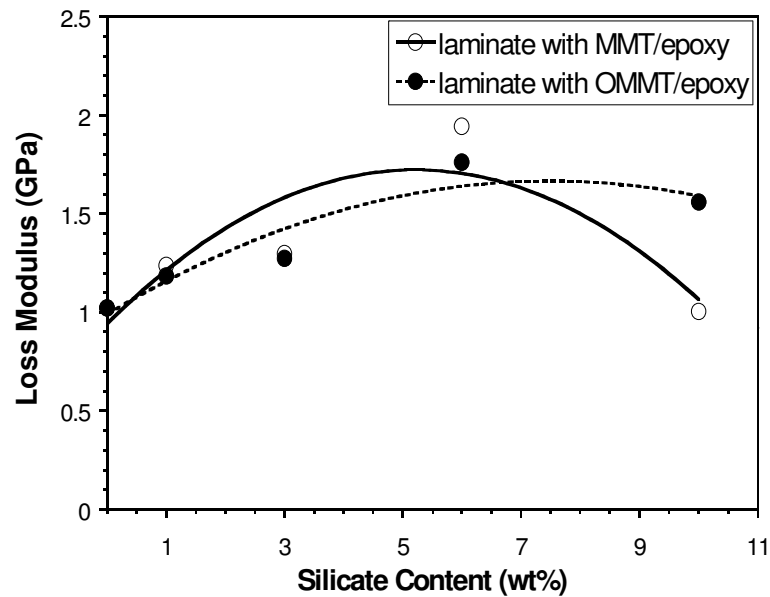


Figure 6.24. Loss modulus of non-crimp fabric reinforced silicate/epoxy nanocomposites

Figure 6.25 shows the effect of silicate loading on the glass transition temperature ( $T_g$ ) of laminates obtained from dynamic mechanical analysis (DMA).  $T_g$  of composites prepared with neat epoxy was measured as 81.9 °C. Addition of MMT particles slightly increases the  $T_g$  of the laminates by 3% up to the concentration of 3 wt.% and further addition reduces the  $T_g$ . The reduction is 6% (from 81.9 °C to 76.8 °C) with the addition of 10 wt. % MMT. This may be related with the void content and the agglomerated structure of unmodified silicate layers at higher silicate concentration. Contrarily, incorporation of OMMT particles increased the  $T_g$  of laminates by 5% (from 81.9 °C to 86.2 °C) with the addition of 10 wt. % OMMT. This improvement is due to the restricted mobility of polymer molecules that was similarly observed in DSC analysis. The  $T_g$  values obtained from DSC and DMA were not same because of the sensitivity difference between these methods. DMA measurements are more sensitive than DSC measurements.

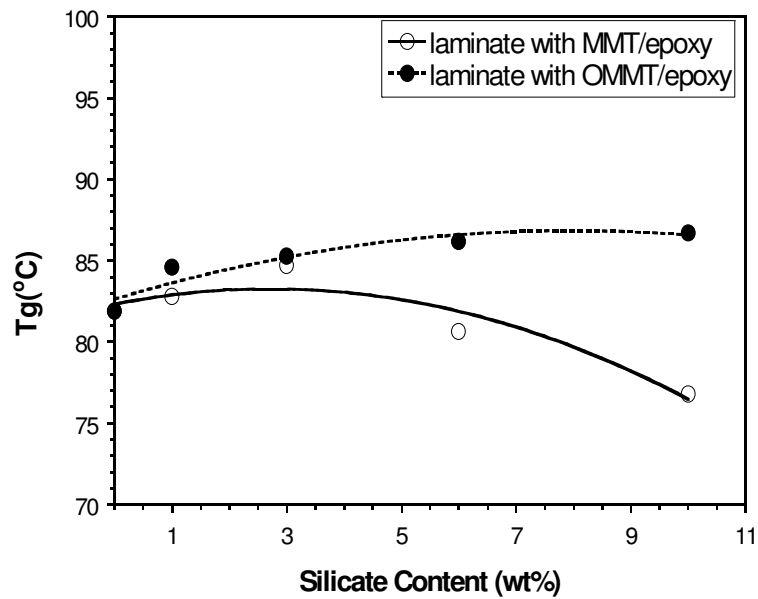


Figure 6.25.  $T_g$  of non-crimp glass fabric reinforced silicate/epoxy nanocomposites obtained by DMA

Similarly, Lin et al. (Lin et al. 2006) applied DMA analysis to the layered silicate/glass fiber/epoxy composites and reported that introduction of silicate increases the  $T_g$  by restricting the mobility of epoxy molecules. Contrarily, Kornmann et al. (Kornmann et al. 2005) reported that the presence of organosilicate in the matrix of glass fiber reinforced composites causes a decrease of glass transition temperature of 10-15 °C. They related this to a cation exchange between the surface modifier of the layered silicate and the curing agent.

## 6.5. Flammability Behaviour of Composites

UL-94 test was applied to the laminates in order to investigate the flammability behaviour of glass fiber/epoxy composites with the addition of modified and unmodified silicate particles. Average extent of burning and average time of burning values were obtained by horizontal burning test (UL94) and the results are given in Figures 6.26 and 6.27, respectively. None of the specimens have burned completely under the test condition. Average extent of burning of the samples obtained from the laminates manufactured with neat epoxy was 45 mm, and addition of modified and unmodified clay particles (10 wt.%) reduced this value to 10 mm and 6 mm,

respectively. Similarly the average time of burning was reduced with the addition of 10 wt.% MMT and OMMT particules from 287 seconds to 129 and 92 seconds, respectively. As it can be clearly seen in Figures 26 and 27, addition of silicate significantly reduced the flammibility of polymer composites and the reduction in average extent of burning and average time of burning is by 55 and 77 %, respectively, due to the addition of 10 wt. % MMT into the epoxy. This improvement is even higher with surface treated silicate (OMMT) due to its better dispersion in the polymer matrix. Addition of OMMT particules reduced average extent of burning by 87% and average time of burning by 68%.

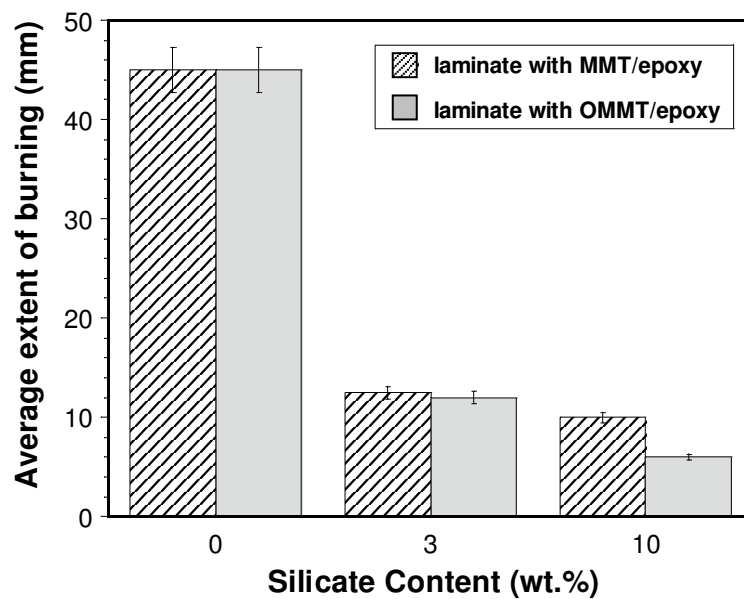


Figure 6.26. Influence of silicate loading on the average extent of burning of the fabric reinforced silicate/epoxy nanocomposites

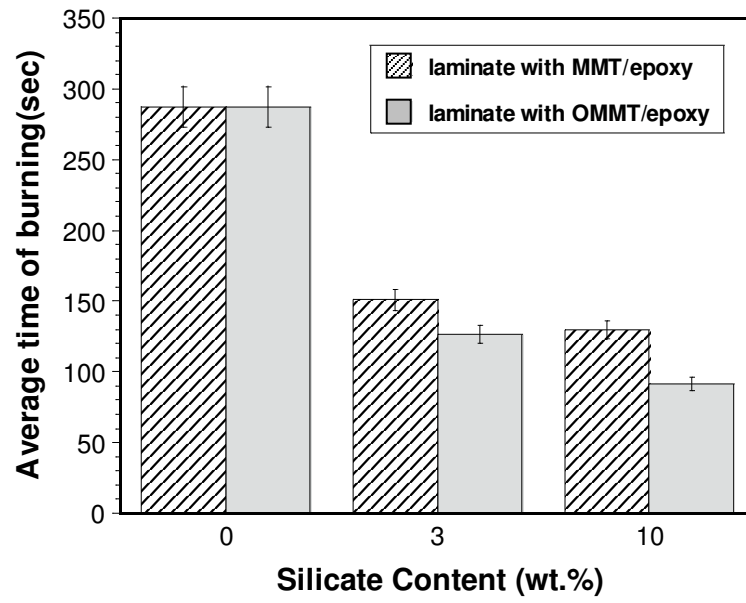


Figure 6.27. Influence of silicate loading on the average time of burning of the fabric reinforced silicate/epoxy nanocomposites

## CHAPTER 7

### CONCLUSIONS

In this study, the effects of modification of the matrix material by the incorporation of silicate nanoparticles on the mechanical, thermal and flame retardant properties of the non-crimp E-glass fiber reinforced epoxy composite systems were investigated.

OMMT particles were obtained by modifying the surface of MMT particles with a HTAC solution. Na<sup>+</sup> ions between the silicate layers were exchanged with alkylammonium cations which makes the hydrophilic surface of silicates organophilic. X-ray analysis of surface treated (OMMT) and untreated (MMT) silicates revealed that the modification of silicate increased the d-spacing of silicate layers that ease the dispersion of silicate particles in the matrix. The d-spacing of silicate layers increased from 14.3Å to 18.1Å with surface treatment process due to intercalation. The characteristic peaks of silicates can not be seen in the XRD diffractograms of glass fiber reinforced laminates due to the further intercalation of silicates during polymerization.

Silicate/epoxy nanocomposite suspensions were synthesized with different concentrations of unmodified (MMT) and modified (OMMT) silicates through in-situ polymerization and were successfully used as matrix resin in non-crimp glass fabric reinforced polymer composites. Fabric reinforced composites were successfully fabricated with silicate/epoxy nanocomposites matrix by hand lay-up technique and cured at room temperature under the pressure of 8 KPa. Fiber volume fractions were measured about 40-44 % for all laminates. The void content of laminates increases with the addition of silicate and this increase was higher with the addition of surface treated ones due to the presence of surfactant material used for surface treatment of silicate particles. The tensile strength and modulus values remain almost constant by the addition of MMT and OMMT up to 6 wt.% silicate contents as compared to those fabricated without silicate addition. However, further addition of MMT and OMMT reduces the strength values. On the other hand, tensile modulus values are reduced by the addition of OMMT while they remains constant with MMT addition at 10 wt.%

silicate loading. Flexural strength and modulus increases with the addition of MMT and OMMT silicate, up to 6 wt. % of silicate loading. Maximum improvement in flexural strength and modulus was obtained at 6 wt. % silicate content and by the addition of nanoparticulates the flexural strength and modulus were improved by 16% and 13%, respectively. Apparent interlaminar shear strength (ILSS) of fabric reinforced composites with neat epoxy matrix was measured as 32.7 MPa. With the addition of silicate, ILSS of laminates decreased slightly and the reduction was greater in the case of OMMT particules addition. The addition of OMMT (10 wt. %) particules to the matrix, increased the fracture toughness of laminates by 5 %. However, the presence of MMT particules slightly reduces  $K_{IC}$  values. The fracture surface examinations revealed that, in the case of composites laminated with silicate containing epoxy matrix, it was evident that fracture mechanisms are altered due to presence of silicates. Addition of MMT particules to the matrix had almost no effect on the  $T_g$  values and  $T_g$  of the laminates increased by 7 % up to 6 wt.% OMMT silicate content. According to DMA results, addition of silicate particules to the matrix increased the storage and loss modulus of composites and  $T_g$  of composites increased with the addition of OMMT particules. Addition of silicate significantly reduced the flammibility of polymer composites and average extent of burning and average time of burning is reduced by 55 % and 77 % due to the addition of 10 wt. % MMT into epoxy. This improvement was even higher with surface treated silicate (OMMT) due to its better dispersion in the polymer matrix. Addition of OMMT particules reduced average extent of burning by 87 % and average time of burning by 68%.

In summary, modification of the matrix network by the incorporation of silicate nanoparticules has no major improvements on the mechanical properties of the non-crimp fabric reinforced epoxy composites. It was found that the effect is the highest on the flexural mechanical properties. Silicate addition has almost no effect on the  $T_g$  with MMT, but is increased by 7 % with OMMT. However, the flame retardancy behaviour that is very critical for polymer composite is significantly improved by the silicate incorporation.

In future studies, layered silicates may be modified by using different types of alkyl ammonium surfactants and layered silicate/epoxy nanocomposites which will be used as the matrix material of fiber reinforced epoxy composites may be produced by shear mixing method to contribute the intercalation of layered silicates.

## REFERENCES

- Adden, S., Horst, P. 2006. "Damage propagation in non-crimp fabrics under bi-axial static and fatigue loading", *Composites Science and Technology*, Vol. 66, pp. 626-633.
- Ahmadi S. J., Huang Y. D. and W. Li. 2004. "Review: Synthetic Routes, Properties and Future Applications of Polymer-layered Silicate Nanocomposites", *Journal of Materials Science*, Vol. 39, pp. 1919 – 1925.
- Ajayan, P. M., Schadler L. S. and Braun P. V., 2003. *Nanocomposite Science and Technology*, (Wiley-VCH, Newyork, USA).
- ASM International, 1987. *Engineered Materials Handbook-Composites*, (Metals Park,Ohi), Vol.1, pp.250-350
- Bibo, G. A., Hogg P. J., 1997. "Influence Of Reinforcement Architecture on Damage Mechanisms and Residual Strength of Glass-Fibre/Epoxy Composite Systems", *Composites Science and Technology*, Vol. 58, pp. 803-813.
- Callister,W. 2000. *Materials Science and Engineering: An Introduction*, (John Wiley & Sons, New York), pp. 85-135
- Chen C., Khobaib M. and Curliss D. 2003. "Epoxy layered-silicate nanocomposites", *Progress in Organic Coatings*, Vol. 47, pp. 376-383.
- Chen K.H. and Yang S.M. 2002, "Synthesis of Epoxy-Montmorillonite Nanocomposite" *Journal of Applied Polymer Science*, Vol. 86, pp. 414-421.
- Chowdury, F.H., Hosur, M. V., Jeelani S. 2006. "Studies on the flexural and thermomechanical properties of woven carbon/nanoclay- epoxy laminates", *Materials Science and Engineering A*, Vol. 421, pp. 298-306
- Dawson, D. K., Brosius, D., Griffiths B., Mason, K.F., Nelson, J., Pottish N. 2006 "High Performance Composites Sourcebook", pp.16-21.
- Dean, D., Walker, R., Theodore, M., Hampton, E., Nyairo, E. 2005. "Chemorheology and preproperties of epoxy/layered silicate nanocomposites", *Polymer*. Vol. 46 pp. 3014-3021.
- Drapier S., Wisnom M.R. 1999. "Finite-element investigation of the compressive strength of non-crimp-fabric-based composites", *Composites Science and Technology*, Vol. 59, pp. 1287-1297.
- Fereshteh-Saniee, F., Majzoobi, G.H., Bahrami, M. 2005. "An experimental study on the behaviour of glass-epoxy composite at low strain rates", *Journal of Materials Processing Technology*. Vol. 162-163 pp. 39-45.

- Giannelis, E. P., 1998. "Polymer Layered Silicate Nanocomposites: Synthesis, Properties and Applications", *App. Organometal. Chem.* Vol. 12, pp. 675-680.
- Gojny, F. H., Wichmann, M. H. G., Fiedler, B., Bauhofer, W., Schulte, K. 2005. "Influence of nano-modification on mechanical and electrical properties of conventional fibre-reinforced composites", *Composites: Part A.* Vol. 36, pp. 1525-1535
- Hackman, I., Hollaway, L. 2006. "Epoxy-layered silicate nanocomposites in civil engineering", *Composites: Part A.* Vol. 37, pp. 1161-1170.
- Hillermeier, R.W., Seferis, J.C. 2001. "Interlayer toughening of resin transfer molding composites", *Composites: Part A.* Vol.32, pp. 721-729.
- Hull, D., Clayne T. W. 1996. *An Introduction to Composites Materials*, (Cambridge University Press, Cambridge), p.12-20.
- Jang, B.Z., 1994. *Advanced polymer composites*, (ASM International Materials Park), p.135
- Jiankun L., Yucal K., Zongneng Q. and Su Y.X. 2000. "Study on Intercalation and Exfoliation Behaviour of Organoclays in Epoxy Resin", *Journal of Polymer Science Part B: Polymer Physics.* Vol. 39, pp. 115-120.
- Jinlian, H., Yi, L., Xueming, S. 2004. "Study on void formation in multi-layer woven fabrics", *Composites: Part A.* Vol. 35, pp. 595-603.
- Jones, R. M. 1975. *Mechanics of composite materials*, (Taylor and Francis), p.45
- Kaya, E. 2006. "*Layered silicate epoxy nanocomposites*", MS. Thesis, İzmir Institute of Technology İzmir, pp.34-68
- Kawasumi M., Hasegawa N., Usuki A. and Okada A. 1998, "Nematic liquid crystal/clay mineral composites", *Materials Science and Engineering C.* Vol.6, pp.135-143.
- Kiuna N., Lawrence C.J., Fontana Q.P.V., Lee P.D., Selerland T., Spelt, P.D.M. 2002. "A model for resin viscosity during cure in the resin transfer moulding process", *Composites: Part A.* Vol.33, pp.1497-1503.
- Kong, H., Mouritz, A.P., Paton, R. 2004. "Tensile extension properties of deformation mechanisms of multiaxial non-crimp fabrics", *Composite Structures.* Vol. 66, pp. 249-259.
- Kornmann X., Lindberg H. and Berglund L.A. 2001, "Synthesis of epoxy-clay nanocomposites:influence of the nature of the clay on structure", *Polymer.* Vol.42, pp.1303-1310.

- Kornmann, X., Rees, M., Thomann, Y., Necola, A., Barbezat, M., Thoman, R. 2005. "Epoxy-layered silicate nanocomposites as a matrix in glass fibre-reinforced composites", *Composites Science and Technology*. Vol. 65, pp. 2259-2268
- Kim, K.Y., Curiskis, J.I., Ye, L., Fu, S.Y. 2005. "Mode-I interlaminar fracture behaviour of weft-knitted fabric reinforced composites", *Composites: Part A*. Vol. 36, pp. 954-964.
- Lee D.C. and Jang L.W. 1998, " Characterization of Epoxy-Clay Hybrid Composite Prepared by Emulsion Polymerization", *Journal of Applied Polymer Science*. Vol. 68, pp. 1997-2005.
- Lin J.C , Chang L.C., Nien M.H.and Ho H.L. 2005, "Mechanical behavior of various nanoparticle filled composites at low-velocity impact", *Composite Structures*. Vol. 32, pp. 982-994
- Lin, L., Lee, J., Hong, C., Yoo, G., Advani. S. G. 2006. "Preparation and characterization of layered silicate/glass fiber/epoxy hybrid nanocomposites via vacuum-assisted resin transfer molding (VARTM)", *Composites Science and Technology*. Vol.66, pp.2116-2125
- Liu W.,i Hoa S.V. and Pugh M. 2005, "Fracture toughness and water uptake of high-performance epoxy/nanoclay nanocomposites", *Composites Science and Technology*. Vol. 65, pp. 2364-2373
- Liu W.,i Hoa S.V. and Pugh M. 2005, "Organoclay-modified high performance epoxy nanocomposites", *Composites Science and Technology*. Vol. 65, pp. 307-316.
- Luo J.J. and Daniel I.M. 2003, "Characterization and modeling of mechanical behavior of polymer/clay nanocomposites", *Composites Science and Technology*. Vol. 63, pp. 1607–1616.
- Meneghetti P.and Qutubuddin S. 2005, "Application of mean-field model of polymer melt intercalation in organo-silicates for nanocomposites", *Journal of Colloid and Interface Science* Vol. 288, pp.387–389.
- Miyagawa, H., Jurek, H., Mohanty, A. K., Misra, M., Drzal, L. T. 2006. "Biobased epoxy/clay nanocomposites as a new matrix for CRFP" *Composites: Part A*. Vol. 37, pp. 54-62.
- Nigam V., Setua V, Mathur G. N. and Kar K.K. 2004, "Epoxy-Montmorillonite Clay Nanocomposites: Synthesis and Characterization", *Journal of Applied Polymer Science*. Vol. 39, pp. 2201-2210.
- Ogasawara, T., Ishida, Y., Ishikawa, T., Aoki, T., Ogura, T. 2006. "Helium gas permeability of montmorillonite/epoxy nanocomposites", *Composites Part A*. Vol. 23, pp. 345-357

- Qutubuddin, S., Fu, X., 2001 *Nano-Surface Chemistry*, (New York, NY, USA), pp. 650-680.
- Ranta D., Manoj N.R., Varley R., Raman R.K.S. and Simon G.P. 2003, “*Clay-reinforced epoxy nanocomposites*”, Society of Chemical Industry. Polym. Int. 0959-8103.
- Ray, S.S., Okamoto M. 2003. “Polymer/layered silicate nanocomposites: a review from preparation to processing”, *Prog. Polym. Sci.* Vol. 28 pp.1539–1641.
- Rouison D., Sain M., Couturier M. 2003. “Resin-Transfer Molding of Natural Fiber-Reinforced Plastic. I. Kinetic Study of an Unsaturated Polyester Resin Containing an Inhibitor and Various Promoters”, *Journal of Applied Science*. Vol. 89, pp. 2553-2561.
- Shahid, N., Villate, R. G., Baron, A. R. 2005. “Chemically functionalized alumina nanoparticle effect on carbon fiber/epoxy composites”, *Composites Science and Technology*. Vol. 27, pp.1123-1131
- Shalin, R.E. 1995. *Polymer matrix composites*, (Chapman-Hall London;New York), p. 256
- Shyr, T.W., Pan Y.H. 2003. “Impact resistance and damage characteristics of composite laminates”, *Composite Structures*. Vol. 62, pp. 193-203.
- Subramaniyan, A. K., Sun, C. T., 2006. “Enhancing compressive strength of unidirectional polymeric composites using nanoclay”, *Composites: Part A*. Vol.12, pp.1454-1462
- Tanoğlu, M., McKnight, S.H., Palmese, G.R., Gillespie Jr., J.W. 2001. “The effects of glass-fiber sizings on the strength and energy absorption of the fiber/matrix interphase under high loading rates”, *Composite Science and Technology*. Vol.61, pp. 205-220.
- Tanoğlu, M., Seyhan., A.T. 2003. “ Investigating the effects of a polyester preforming binder on the mechanical and ballistic performance of E-glass fiber reinforced polyester composites”, *International Journal of Adhesion &Adhesives*. Vol. 23, pp.1-8.
- Tarım, N., Fındık, F., Uzun, H. 2002 “Ballistic impact performance of composite structures”, *Composite Structures*. Vol. 56, pp.13-20.
- Thomassin, J.M., Pagnouille C., Caldarella, G., Germain A., Jerome R. 2006. “Contribution of nanoclays to the barrier properties of a model proton exchange membrane for fuel cell application” , *Journal of Membrane Science*. Vol. 270, pp. 50-56.
- Tong, L., Mouritz, A.P.,Bannister, M.K. 2002 *3D Fibre Reinforced Polymer Composites*, (Elsevier Science), pp. 221-239

- Ulven, C., Vaidya, U.K., Hosur, M.V. 2003. "Effect of projectile shape during ballistic perforation of VARTM carbon/epoxy composite panels", *Composite Structures*. Vol.61, pp. 143-150.
- Vasiliev, V. V. 1993. *Mechanics of composite structures*, (Taylor and Francis, Washington), pp. 127-211
- Verpoest, I., Lomov, S. V. 2005. "Virtual textile composites software WiseTex: Integration with micro-mechanical, permeability and structural analysis", *Composites Science and Technology*, Vol. 65, pp. 2563-2574.
- WEB\_1, 2006. Farmingdale University web site, 17/05/2006, <http://info.lu.farmingdale.edu/depts/met/met205/composites.html>
- WEB\_2, 2006. Composite Reinforcement Fabrics web site, 14/05/2006, <http://www.vectorply.com/reinforcement>.
- WEB\_3, 2006. TWI web site, 19/06/2006, <http://www.twi.co.uk/j32k/protected>
- WEB\_4, 2006. Fire testing web site, 25/06/2006, <http://www.fire-testing.com>
- Yang B., Kozey V., S. Adanur S., Kumar S. 2000. "Bending, compression, and shear behavior of woven glass fiber-epoxy composites", *Composites: Part B*. Vol. 31, pp. 715-721.
- Zhao, L. G., Warrior, N.A., Long, A.C., 2006. "Finite element modelling of damage progression in non-crimp fabric reinforced composites", *Composites Science and Technology*. Vol. 66, pp. 36-50.